

VOL. 34 **INDIAN JOURNAL OF PHYSICS** No. 10

(*Published in collaboration with the Indian Physical Society*)

AND

VOL. 43 **PROCEEDINGS** No. 10

OF THE

**INDIAN ASSOCIATION FOR THE
CULTIVATION OF SCIENCE**

OCTOBER 1960

PUBLISHED BY THE
INDIAN ASSOCIATION FOR THE CULTIVATION OF SCIENCE
JADAVPUR, CALCUTTA 32

BOARD OF EDITORS

K. BANERJEE	D. S. KOTHARI,
D. M. BOSE	S. K. MITRA
S. N. BOSE	K. R. RAO
P. S. GILL	D. B. SINHA
S. R. KHASTGIR,	S. C. SIRKAR (<i>Secretary</i>)
B. N. SRIVASTAVA	

EDITORIAL COLLABORATORS

PROF. D. BASU, PH.D.
PROF. J. N. BHAR, D.Sc., F.N.I.
PROF. A. BOSE, D.Sc., F.N.I.
DR. K. DAS GUPTA, PH.D.
PROF. N. N. DAS GUPTA, PH.D., F.N.I.
PROF. A. K. DUTTA, D.Sc., F.N.I.
DR. S. N. GHOSH, D.Sc.
PROF. P. K. KICHLU, D.Sc., F.N.I.
DR. K. S. KRISHNAN, D.Sc., F.R.S.
PROF. D. N. KUNDU, PH.D.
PROF. B. D. NAG CHOWDHURY, PH.D.
PROF. S. R. PALIT, D.Sc., F.R.I.C., F.N.I.
DR. H. RAKSHIT, D.Sc., F.N.I.
DR. R. GOPALAMURTY RAO
PROF. A. SAHA, D.Sc., F.N.I.
DR. VIKRAM A. SARABHAI, M.A., PH.D.
DR. A. K. SENGUPTA, D.Sc.
DR. M. S. SINHA, D.Sc.
PROF. N. R. TAWDE, PH.D., F.N.I.
DR. P. VENKATESWARLU

Assistant Editor

DR. MONOMOCHAN MAZUMDER, D. PHIL.

Annual Subscription—

Inland Rs. 25.00

Foreign £ 2-10-0 or \$ 7.00

NOTICE TO INTENDING AUTHORS

Manuscripts for publication should be sent to the Assistant Editor, Indian Journal of Physics, Jadavpur, Calcutta-32.

The manuscripts submitted must be type-written with double space on thick foolscap paper with sufficient margin on the left and at the top. The original copy, and not the carbon copy, should be submitted. Each paper must contain an ABSTRACT at the beginning.

All REFERENCES should be given in the text by quoting the surname of the author, followed by year of publication, *e.g.*, (Roy, 1958). The full REFERENCE should be given in a list at the end, arranged alphabetically, as follows; ROY, S. B., 1958, *Ind. J. Phys.*, **32**, 323.

Line diagrams should be drawn on white Bristol board or tracing paper with black Indian ink, and letters and numbers inside the diagrams should be written neatly in capital type with Indian ink. The size of the diagrams submitted and the lettering inside should be large enough so that it is legible after reduction to one-third the original size. A simple style of lettering such as gothic, with its uniform line width and no serifs should be used, *e.g.*,

A·B·E·F·G·M·P·T·W·

Photographs submitted for publication should be printed on glossy paper with somewhat more contrast than that desired in the reproduction, and should, if possible, be mounted on thick white paper.

Captions to all figures should be typed in a separate sheet and attached at the end of the paper.

The mathematical expressions should be written carefully by hand. Care should be taken to distinguish between capital and small letters and superscripts and subscripts. Repetition of a complex expression should be avoided by representing it by a symbol. Greek letters and unusual symbols should be identified in the margin. Fractional exponents should be used instead of root signs.

Bengal Chemical and Pharmaceutical Works Ltd.

The Largest Chemical Works in India

Manufacturers of Pharmaceutical Drugs, Indigenous Medicines, Perfumery Toilet and Medicinal Soaps, Surgical Dressings, Sera and Vaccines Disinfectants, Tar Products, Road Dressing Materials, etc.

Ether, Mineral Acids, Ammonia, Alum, Ferro-Alum Aluminium Sulphate, Sulphate of Magnesium, Ferri Sulph. Caffeine and various other Pharmaceutical and Research Chemicals.

Surgical Sterilizers, Distilled Water Stills, Operation Tables, Instrument Cabinets and other Hospital Accessories.

Chemical Balance, Scientific Apparatus for Laboratories and Schools and Colleges, Gas and Water Cocks for Laboratory use Gas Plants, Laboratory Furniture and Fittings.

Fire Extinguishers, Printing Inks.

Office: **6, GANESH CHUNDER AVENUE, CALCUTTA-13**

Factories: **CALCUTTA - BOMBAY - KANPUR**

B O R O S I L

LABORATORY GLASSWARE

such as

FLASKS, BEAKERS, CONDENSERS, MEASURING FLASKS, MEASURING CYLINDERS, PIPETTES & ANY SPECIAL APPARATUS MADE TO DESIGN

and

PENICILIN VIALS, VACCINE BULBS—WHITE & AMBER

•
ALL OTHER APPARATUS & EQUIPMENT MANUFACTURED TO CLIENT'S DESIGN

**INDUSTRIAL & ENGINEERING APPARATUS CO.
PRIVATE LIMITED**

CHOTANI ESTATES, PROCTOR ROAD, GRANT ROAD, BOMBAY 7

New Dual-Trace DG to 15 MC TYPE 516 OSCILLOSCOPE

GENERAL DESCRIPTION

The Type 516 is a dual-trace semi-ruggedized oscilloscope using frame-grid tubes for reliability. It handles applications in the dc to 15mc range. Vertical deflection factor is 0.05 v/div for each channel, with four operating modes possible. Small size and light weight combined with simple operation and reliable performance fit the dual-trace Type 516 Oscilloscope for many laboratory and field applications.

TEKTRONIX CATHODE-RAY TUBEg

Flat-faced 5-inch crt provides bright trace. Accelerating potential is 4 kv.

DC-coupled unblanking of the beam.

External crt cathode terminal permits beam intensity modulation.

Phosphor normally supplied is a P2, but a P1, P7, or P11 will be supplied if requested.

Usable viewing area is 6 by 10 centimeters.

Graticule has adjustable edge-lighting.

AMPLITUDE CALIBRATOR

11 steps from 0.05 to 100 volts peak-to-peak. Accuracy of the voltage settings are within 3%. Square-wave frequency is approximately 1 kc.

Output Waveforms

150 volts peak-to-peak (approximate amplitude) from SAWTOOTH OUT connector.

30 volts peak-to-peak (approximate amplitude) from +GATE OUT connector.

The vertical-deflection system of this new Dual-Trace Oscilloscope has four operating modes: (1) Input channels switched on alternate sweeps—(2) Input channels switched at a free-running rate of about 150 kc—(3) Channel A used separately—(4) Channel B used separately. It is a completely-integrated highquality laboratory oscilloscope with the additional advantages of small size, low weight, high reliability, and easy operation.

For particulars. Please write to :

ELECTRONIC ENTERPRISES

46, Karani Building,

Opposite Cama Baug.

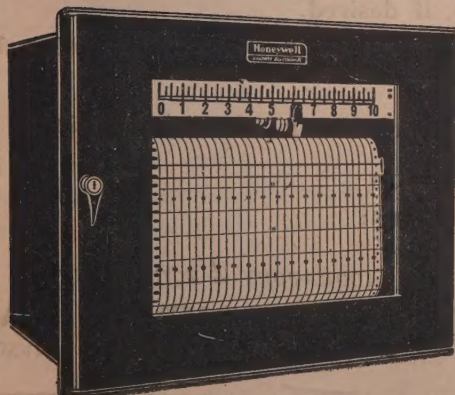
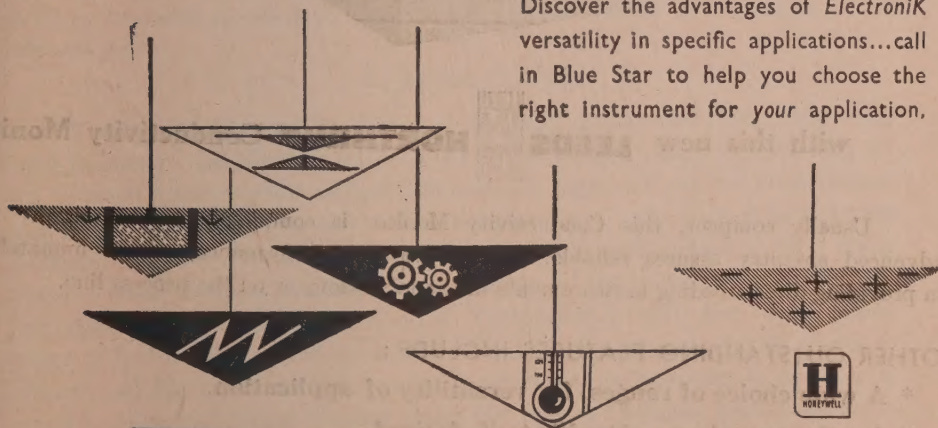
NEW CHARNI ROAD, BOMBAY-4.

The
ElectroniK
recorder
or indicator
is a
thousand
instruments
in one

An *ElectroniK* instrument adapts easily to your changing needs, never becomes obsolete. Its remarkable versatility is made possible by the many measuring circuits...many types of records or indications...many pen or print wheel speeds...and the wide variety of functions that can be incorporated in the instrument.

Use *ElectroniK* instruments to measure temperature, pressure, flow, pH, chemical concentration, voltage, speed — any variable that's translatable into a d-c signal.

Discover the advantages of *ElectroniK* versatility in specific applications...call in Blue Star to help you choose the right instrument for your application.



Honeywell

First in Control

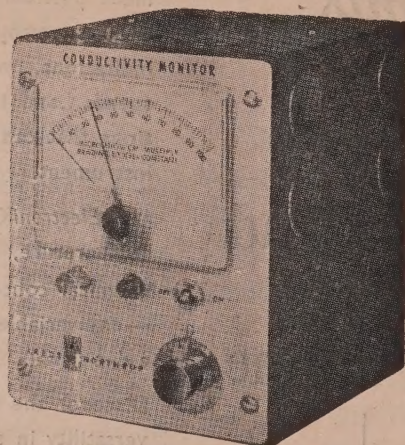
Sold and serviced in India exclusively by


BLUE STAR

**BLUE STAR ENGINEERING
CO. (Calcutta) Private LTD.**
7 HARE STREET, CALCUTTA 1

Also at BOMBAY • DELHI • MADRAS

Now . . . measure **SOLUTION CONDUCTIVITY** continuously



with this new **LEEDS**  **NORTHROP** Conductivity Monitor

Usually compact, this Conductivity Monitor is completely transistorized. Its advanced circuitry assures reliable, maintenance-free performance. It is unmatched in providing direct-reading measurements in the laboratory or on the process line.

OTHER OUTSTANDING FEATURES INCLUDE :

- * A wide choice of ranges, for versatility of application.
- * Continuous alarm signalling, if desired.
- * An output d-c signal for transmission to a recorder or other data-logging equipment.
- * Light-weight portable model with handle for easy carrying.

For further particulars please write to :

SOLE DISTRIBUTORS FOR LABORATORY & EQUIPMENT

THE SCIENTIFIC INSTRUMENT COMPANY LIMITED

ALLAHABAD, BOMBAY, CALCUTTA, MADRAS, NEW DELHI

AN ISOTOPE EFFECT IN THE COLLECTION ON CHARGED PLATES OF (n, γ) RECOIL PRODUCTS OF BROMINE

H. J. ARNIKAR AND A. LAL

LABORATORY OF NUCLEAR AND PHYSICAL CHEMISTRY, BANARAS HINDU UNIVERSITY, BANARAS

(Received, June 16, 1960)

ABSTRACT. A study of the relative yields of Br^{80} , Br^{80m} and Br^{82} following an irradiation of $\text{C}_6\text{H}_5\text{Br}$ for a duration of 9 days, by an analysis of the time-decay curves, show that the apparent yield of Br^{80} on the anode plate is roughly twice that of Br^{82} . These results are discussed, *vis-a-vis*, standard data for the thermal neutron capture cross sections of corresponding target atoms, Br^{79} and Br^{81} and their relative abundances. These findings, considered along with the probable counting efficiency for the resulting radioactive products and their decay characteristics, point to the existence of a small but definite net isotope effect in the overall process of (i) recoil, (ii) charge acquisition, and (iii) collection on the charged plate.

INTRODUCTION

Results of early workers (Fermi *et al.*, 1935; Libby and Vault, 1939, 1941 and Goldsmith and Bluerer, 1950) on the use of charged plates for collecting the (n, γ) recoil products show marked differences in respect of relative yields collecting on the plates of either sign and of a separation or otherwise of isotopic and isomeric products. Fermi *et al.* (1935) found in the case of methyl or ethyl iodide vapour under neutron irradiation, the polarity of the collecting electrode was not significant. Similarly Libby and de Vault (1939 & 1941) find equal enrichment of Br^{80} isomers on the anode and cathode. On the contrary, the results of Paneth and Fay (1935 and 1936) on the separation of radioisotopes of As as well as of bromine and iodine forming under the Szilard-Chalmers' process showed a marked dependence of the yield not only on the sign of the electrode but on its chemical nature and physical condition of the surface. With Pt electrodes, for instance, no activity collects in the case of irradiation of aliphatic halogen compounds, while with smooth Ag or Cu electrodes the active products are deposited exclusively on the anode. In the case of bromobenzene, however, products collect on both anode and cathode in the ratio of roughly 2:1. The results of Capron (1946) are at further variance, more activity collects on the cathode than on the anode in the case of $\text{C}_2\text{H}_4\text{Br}_2$, while it is the reverse in the case of $\text{C}_6\text{H}_5\text{Br}$. This last finding of preferential collection on the anode appears to be of more frequent occurrence as, for instance, also in the separation of In^{114} isomers (Goldsmith and Bluerer, 1950).

There is a similar lack of agreement in respect of whether or not an isotopic and isomeric enrichment occurs in the products of the recoil process collecting on the charged plates. Fox and Libby (1952) Roul and Libby (1953) and Chien and Willard (1954) find no isotopic effect in the retention (fraction of active products left in the original organic medium unrecovered) in the case of *iso*- and *n*-propyl bromide, while Shaw (1951 and 1956) as well as Capron and co-workers (1946, 1952 and 1953) find important isotopic and even isomeric effects at least in the case of aromatic bromo-compounds. No agreed mechanism is available for the secondary reactions following the (n, γ) recoil reaction, to account for the relative yields on the charged plates of the different isotopic and isomeric products as in the case of bromobenzene. The following work has been undertaken with the object of obtaining experimental data under controlled conditions which would help in understanding the role of ionization in the above, an aspect relatively less studied hitherto. The present paper reports results for the collection on charged plates of radioisotopes of bromine in a state of high specific activity and of the associated isotope effect.

EXPERIMENTAL

About 500 ml of bromobenzene were irradiated in a pyrex beaker by a 50mC source of (Ra+Be) plunged in the liquid. The neutron source was surrounded by 2 cm of paraffin and a thin walled glass tube. This glass sheath was necessary as both paraffin and polythene were found to be acted upon by bromobenzene under the action of the accompanying high energy gamma radiation. The

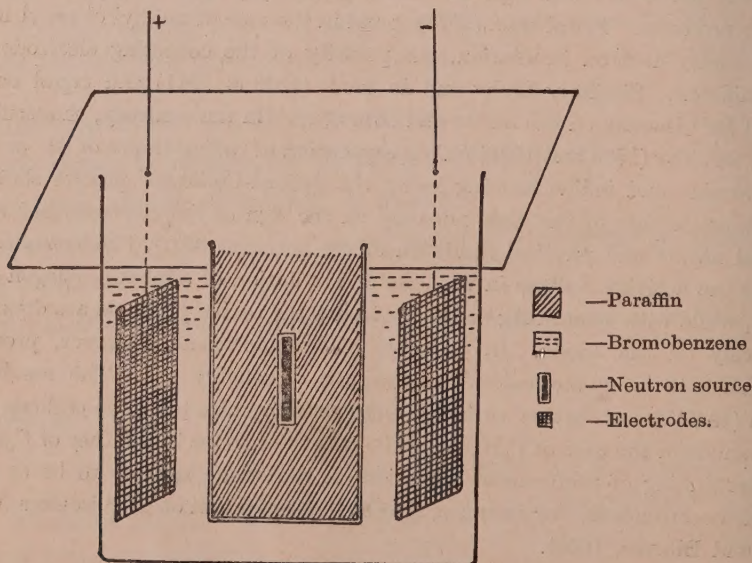


Fig. 1. Arrangement for the collection of (n, γ) recoil products of bromine on charged plates.

electrodes consisting of two parallel plates of either (1) copper with a thin coat of agar-agar gel containing 0.1% of NaOH or (2) silver with or without a trace of AgBr, were placed 6 cms apart and symmetrically with respect to the neutron source, as shown in Fig. I. The field was provided by a battery of 90 volts connected across the electrodes. Irradiations were conducted for a period of 9 days corresponding to about six-times the half-life of the longest lived isotope, viz. 36 hr Br-82. Sometimes a field of 1050 volts was applied during the last 5 hours of irradiation. The radio-isotopes were recovered in the end from the two charged plates separately as follows. In the case of the gel-coated copper electrodes, the gel was melted by warming and the liquid collected was evaporated directly in a counting tray and in the case of the Ag electrodes, the isotopes were recovered by washing the surface with a small amount of ammonia and evaporating the liquid to dryness in a counting tray. Separated in this way, the product was in a state of high specific activity, the amount of inactive bromine being inappreciable.

RESULTS

The activities collected on the positive and negative electrodes were measured separately with a thin end-window G. M. counter under conditions of constant geometry. From an analysis of the corresponding time-decay curves the relative yields of different radioisotopes present in the fraction collected were computed. From two measures of the total activity produced in the liquid, with and without the electric field, determined with a liquid counter, the percentage retention was calculated. This varied between 60 to 70% for all the isotopes considered together. Decay curves (Figs. 2 and 3) which are typical of numerous observations show that three activities Br-82 (36 hr) and the metastable Br-80_m (4.4hr) and her ground state Br-80 (18 min) are produced. Also some of the last activities were directly formed from the target Br-79.

The use of extremely thin end-window counter permitted the counting of 80 KeV gammas, of which about 45% are internally converted, with an efficiency comparable to the counting of the betas from Br-80 and Br-82. Countings with a scintillation counter with and without filters for the betas justified this.

The relative yields given in Table I of the different activities collecting on the two electrodes are typical of a series of experiments.

TABLE I

Activity	Anode	Cathode
Total	450	220
36-hour	115	88
18-min	200	100
4.4-hour	135	32

The periods of the two isomers are such that they reach transient equilibrium during the duration of the experiment and the shorter lived (18 min) Br-80 decays with the same period, *viz.*, 4.4 hours as its parent Br-80*m*. Hence of the total 4.4. hour activity measured one half is due to the daughter product,

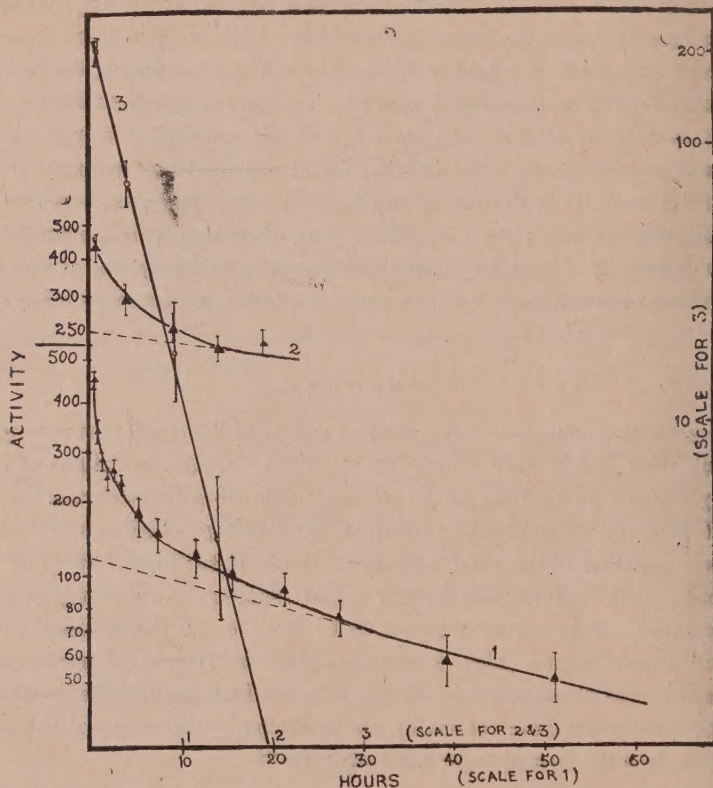


Fig. 2. Analysis of the decay curves of the activity collecting on the anode.
Positive Plate 1. Decay curve - Br-80, Br-80*m*, Br-82, 2. Decay curve : Br-80 & Br-80*m*,
3. Half-life line : Br-80.

This 'half' value together with the 18 min. activity directly formed from the target represents the total Br-80 collected. Table II shows the net values of the different radiostopes directly formed from the target.

TABLE II

Isotope	Anode	Cathode
Br-82	115	88
Br-80	200	100
Br-80 <i>m</i> .	68	16

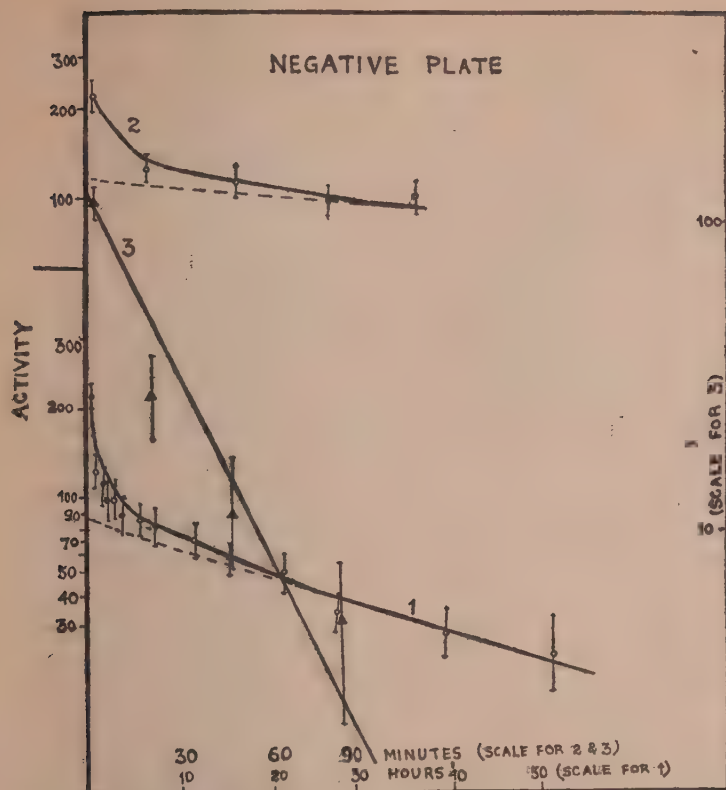


Fig. 3. Analysis of the decay curve of the activity collecting on the anode.

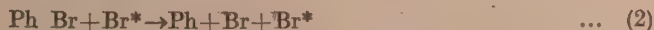
1. Decay curve: Br-80, Br-80m & Br-82, 2. Decay curve: Br-80 & Br-80m, 3. Half-life line: Br-80.

DISCUSSION

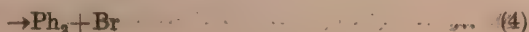
In the formation of Br-80 by the (n, γ) reaction the maximum energy of the gamma emitted is 7.88 MeV (Groshev *et al.*, 1959) which gives 416 eV as the corresponding maximum recoil energy of the Br-80 nucleus, which is adequate for its rupture from the parent molecule. The initial recoil-rupture reaction



is, according to Libby (1947), followed by



As a recombination of these high energy particles may not be readily possible, Shaw (1956) suggests the following secondary reactions:



Reactions (3) and (4) tend to increase the Szilard-Chalmers' extraction yield while the isotope exchange reaction Eq.(5).



leads to increased retention. This is the basis of concentrating radioisotopes by the Szilard-Chalmer technique.

In the above mechanism, it is to be noted, that ionization is not referred to as a necessary stage. As against this, the results presented above as well as those reported earlier by Capron *et al* (1958) point to the appearance of ionization at some stage in the process. In our experiment, both positively and negatively charged particles have been collected (*vide* Table II). With a high factor of internal conversion ($\sim 45\%$) associated with the transition $\text{Br-80} \rightarrow \text{Br } 80m$, a fraction of the initially formed Br-80 is to be expected to be in the Br^+ state, following considerable electron loss due to Auger effect. This accumulation of charge, Goldsmith and Bluerer (1950) have shown, may lead to molecular dissociation. Earlier, Cooper (1942) had worked out the theoretical basis for the occurrence of such molecular dissociations occurring as a consequence of the Franck-Condon principle.

These considerations account for the positively charged particles collecting on the cathode and of the concentration of the ground state isomer Br-80 on the cathode. The extreme instability of the Br^+ , however, leads to a greater fraction of it to be changed to Br^- finally during transit through the bromobenzene medium. A value of 5.4 for the dielectric constant of the medium is considered high enough to bring about this conversion. These results finally lead to a greater yield on the anode than on the cathode as observed. It is clear that other modes of ionization have to be contemplated, in addition to the Auger consequence following internal conversion, for explaining the collection on charged plates of the metastable isomer and, more specially the isotope Br-82 which does not undergo isomeric transition.

The other observation of interest is the occurrence of an isotope effect in the relative yields of the radio-isotopes Br-80, Br-80 m and Br-82 collecting on either electrode. The relative yield (γ) for a given species is directly related to the capture cross-section (σ) of the corresponding target nucleus and its amount (n) in the path of the neutron beam. We may thus write for the yield,

$$\gamma_i = \theta_i \sigma_i n_i$$

Here θ is the fraction of the given product finally collecting on a given charged plate. In the absence of an isotope effect this fraction ($\gamma/\sigma n$) should be the same for all the species. Table III shows the relative yields together with known data for the percentage natural abundance (n) and the capture cross-section (σ) of the corresponding target nuclei Br-79 and Br-81.

TABLE III

Target data			Product yields			
			Anode		Cathode	
σ (barns)		$n(\%)$	γ	$\gamma/\sigma n$	γ	$\gamma/\sigma n$
Br-79 (18 min.)	8.5	50.5	200	0.466	100	0.233
Br-79 (4.4 hr.)	2.9	50.5	68	0.466	16	0.109
Br-81	3.5	49.5	115	0.665	88	0.507

Results for the positive plate show the occurrence of a marked isotope effect in the formation and the collection of the isotopes, Br 80 and Br 82, in contrast with its absence as between the two isomers Br-80 *m* and Br-80 as shown by the characteristic $(\gamma/\sigma n)$ values. In the case of the negative plate however, an additional enrichment of the isomers is also apparent. This undoubtedly arises from the predominance of Br⁺ in the ground state of Br-80 following the internal conversion—ionization mechanism discussed above. The value for $(\gamma/\sigma n)$ for Br-80 is over twice that for Br-80 *m* on the negative plate, while the two values are the same for positive plate.

The earlier results of Shaw (1956) indicate a similar order of retention as between the two isomers. Our results however differ from those of Shaw in respect of the order of the yield as between the lighter and heavier isotopes. The formation of active water-soluble compounds, other than HBr and elementary bromine, during accompanying radiolysis is considered one of the causes for the variable yields reported by earlier workers, employing aqueous extraction to concentrate the recoil products. It would thus appear that the method adopted in the present work of collecting the products on dry charged plates would minimize these variables. A more detailed investigation in respect of the influence of field intensity, nature of the target substance and possibly temperature, would be helpful in understanding some of the secondary reactions following the (n, γ) reaction.

REFERENCES

- Capron, 1946, *Nature*, **157**, 806.
 Capron and Oshima, 1952, *J. Chem. Phys.*, **20**, 1403.
 Capron and Crevecoeur, 1952, *J. Chim. phys.*, **49**, 29.
 Capron and Crevecoeur, 1953, *J. Chem. Phys.*, **21**, 1843.
 Capron *et al.*, 1958, Proc. Second Int. Conf. (Peaceful Uses of Atomic Energy), Geneva, Sept., 1958.
 Chien and Willard, 1954, *J. Am. Chem. Soc.*, **76**, 4735.
 Cooper, 1942, *Phys. Rev.*, **61**, 1.
 Fay and Paneth, 1935, *Nature*, **135**, 820.
 Fay and Paneth, 1936, *J. Chem. Soc.*, 384.

- Fermi, Amaldi and others, 1935, *Proc. Roy. Soc.*, A149, 522.
Fox and Libby, 1952, *J. Chem. Phys.*, 20, 487.
Groshev, *et al.*, 1959, "Atlas of γ -Ray Spectra for Radiative Capture of Thermal Neutrons" (Pergamon Press, London).
Goldsmith and Bluerer, 1950, *J. Phys. & Colloid Chem.*, 54, 717.
Libby and de Vault, 1939, *Phys. Rev.*, 55, 322.
Libby and de Vault, 1941, *J. Am. Chem. Soc.*, 63, 3216.
Libby, 1947, *J. Am. Chem. Soc.*, 69, 2523.
Millman and Shaw, 1956, *J. Chem. Soc.*, 2101.
Rouland and Libby, 1953, *J. Chem. Phys.*, 21, 1495.
Shaw, 1951, *J. Chem. Soc.*, 443.
Shaw and Collie, 1951, *J. Chem. Soc.*, 434.

THERMAL DIFFUSION FACTOR FOR HYDROGEN AND WATER MIXTURES

S. C. SAXENA

CHEMISTRY DIVISION, ATOMIC ENERGY ESTABLISHMENT TROMBAY, BOMBAY

(Received, August 1, 1960)

ABSTRACT. The thermal diffusion factor for the system hydrogen and water-vapour, has been calculated from an equation which utilises only the experimental data on transport properties and their temperature derivatives and is independent of any particular form for the inter-molecular potential. The thermal diffusion factor has also been computed for other systems which emerge out of the different isotopic species of these two principal components. These values are of particular interest in interpreting the data obtained on the enrichment of hydrogen isotopes, in a thermal diffusion column, using the following chemical exchange reaction :



INTRODUCTION

Considerable interest centres around the equilibrium and non-equilibrium properties of water and its mixtures with other gases. This is because of the presence of water vapour all around us in the atmosphere and design-engineers need all such data in connection with their problems involving heat transfer etc. References to such data are found in the work of Keenan and Keyes (1954), Hirschfelder, Curtiss and Bird (1954a), Powell (1958), and Liley (1958). In recent years, some success has been achieved in computing the properties of non-polar molecules from the theoretical results of statistical mechanics in conjunction with spherically symmetric intermolecular potentials. Unfortunately, the position for polar molecules is far from satisfactory. For such molecules, the complicated angle-dependent potentials make it very difficult, if not impossible, to calculate the various collision cross-sections. There is an additional interest in the thermal diffusion factor for the hydrogen and water system, for thermal diffusion coupled with chemical exchange has been tried by Pierce (1959) to enrich the hydrogen isotopes in a thermal diffusion column. The theoretical calculations of the thermal diffusion factor, in particular, are more complicated because of the following two reasons : Firstly, the infinite determinants which represent the thermal diffusion factor have been expanded into an infinite series by two different methods, viz., Chapman-Cowling (1952) and Kihara (1949), Mason (1957). Secondly, both these infinite series have in general rather poor convergence and consequently, to arrive at reliable results for actual systems elaborate numerical calculations

have to be performed for the specific intermolecular potential. In this paper all these difficulties have been successfully surmounted and the values of the thermal diffusion factor for the various combinations of the stable isotopes of hydrogen with normal and heavy hydrogen water have been calculated in the temperature range 307°K to 350°K for both the ends of the concentration range.

FORMULAE FOR THE THERMAL DIFFUSION FACTOR

The general formula for the thermal diffusion factor, α_T , is given in the books of Chapman-Cowling (1952) and Hirschfelder, Curtiss and Bird (1954) as the ratio of infinite determinants. Various approximations are then obtained by expanding these infinite determinants according to the procedure of either Chapman-Cowling (1952) or Kihara (1949). Mason (1957) has studied in detail the convergence errors involved in α_T on various intermolecular potentials and for specific types of mixtures. Recently, Weissman, Saxena and Mason (1960) have shown that for a binary mixture, where the heavy component is in trace and the ratio of the molecular masses $\simeq 0.1$ or less, α_T can be calculated within one to two percent by the following formula:

$$[\alpha_T] = (6C_{12}^* - 5)(-S_2/Q_2)(1+K), \quad \dots (1)$$

where the subscript 2 represents the lighter component and for a mixture consisting of polar and nonpolar components (being designated by the subscripts p and n respectively) we have:

$$-S_2 = -S_n = \frac{15M_p(M_p - M_n)}{2(M_p + M_n)^2} + \frac{4M_p M_n A_{p-n}^*}{(M_p + M_n)^2} - \frac{M_n}{M_p} \left(\frac{2M_n}{M_n + M_p} \right)^{\frac{1}{2}} \left(\frac{\sigma_{n-n}^2 \Omega_{n-n}^{(2,2)*}}{\sigma_{p-n}^2 \Omega_{p-n}^{(1,1)*}} \right), \quad \dots (2)$$

$$Q_2 = Q_n = \frac{2}{M_p(M_p + M_n)} \left(\frac{2M_p}{M_p + M_n} \right)^{\frac{1}{2}} \left(\frac{\sigma_{n-n}^2 \Omega_{n-n}^{(2,2)*}}{\sigma_{p-n}^2 \Omega_{p-n}^{(1,1)*}} \right) (3M_p^2 + M_n^2 + (8/5)M_p M_n A_{p-n}^*), \quad \dots (3)$$

$$A_{p-n}^* = \Omega_{p-n}^{(2,2)*} / \Omega_{p-n}^{(1,1)*}, \quad \dots (4)$$

$$C_{12}^* = C_{p-n}^* = \Omega_{p-n}^{(1,2)*} / \Omega_{p-n}^{(1,1)*}, \quad \dots (5)$$

$$K = \frac{1}{42} (8E_{n-n}^* - 7)^2 + \frac{2}{21} \left(1 - \frac{M_n}{M_p} \right) (8E_{n-n}^* - 7) [1 - \frac{3}{4} (5 - 4B_{p-n}^*)(6C_{p-n}^* - 5)^{-1}], \quad \dots (6)$$

$$B_{p-n}^* = [5\Omega_{p-n}^{(1,2)*} - 4\Omega_{p-n}^{(1,3)*}] / \Omega_{p-n}^{(1,1)*}, \quad \dots \quad (7)$$

$$E_{n-n}^* = \Omega_{n-n}^{(2,3)*} / \Omega_{n-n}^{(2,2)*} \quad \dots \quad (8)$$

where M represents the molecular mass, $\Omega^{(i,j)*}$ are the reduced Chapman-Cowling collision integrals and σ is the collision diameter. Here, we have arbitrarily chosen the subscript 2 for the nonpolar component, hydrogen, in order to be consistent with the convention of assigning the subscript 1 to the heavier component. In case, the lighter component is polar, correct values will be obtained, if the subscripts representing the molecular species are interchanged.

A straightforward calculation of α_T is not possible from these expressions, for the various collision cross-sections have not been evaluated for such an intermolecular potential which takes into account the polar nature of the molecules. The labour involved in the evaluation of these collision integrals is formidable and as yet this has not been accomplished. However, all these collision integrals (except A_{p-n}^*) can be replaced by the absolute values of the transport coefficients or their temperature derivatives. The required relations are:

$$(6C_{p-n}^* - 5) = 2 \left[2 - \left(\frac{\partial \ln D_{p-n}}{\partial \ln T} \right)_{pr} \right], \quad \dots \quad (9)$$

$$(5 - 4B_{p-n}^*) = 5 - \frac{1}{3} \left[2 \left(\frac{\partial \ln D_{p-n}}{\partial \ln T} \right)_{pr} - 1 \right] \\ \left[9 - 2 \left(\frac{\partial \ln D_{p-n}}{\partial \ln T} \right)_{pr} \right] - \frac{4}{3} \frac{d^2 \ln D_{p-n}}{d(\ln T)^2}, \quad \dots \quad (10)$$

$$(8E_{n-n}^* - 7) = 2 \left[1 - \frac{\partial \ln \eta_{n-n}}{\partial \ln T} + \frac{\partial \ln f_n}{\partial \ln T} \right], \quad \dots \quad (11)$$

$$-S_n = \frac{15M_p(M_p - M_n)}{2(M_p + M_p)^2} + \frac{4M_p M_n A_{p-n}^*}{(M_p + M_n)^2} - \frac{5}{3} \frac{M_n^2}{(M_p + M_n)} \frac{p D_{p-n} f \eta}{\eta_{n-n} R T}, \quad \dots \quad (12)$$

$$Q_n = \frac{10}{3} \frac{M_n}{(M_n + M_p)} \left(\frac{pr D_{p-n}}{\eta_{n-n} R T} \right) \left((3M_p^2 + M_n^2 + \frac{8}{5} M_p M_n A_{p-n}^*) \right), \dots \quad (13)$$

$$f\eta = 1 + \frac{3}{196} (8E_{n-n}^* - 7). \quad \dots \quad (14)$$

In the above equations pr stands for the pressure. When the light component is in trace following Mason (1957) α_T can be calculated thus:

$$\alpha_T = \left[2 - \left(\frac{\partial \ln D_{p-n}}{\partial \ln T} \right)_{pr} \right] \left[1 - \mu_1 \left(\frac{M_n}{M_p} \right) \right], \quad \dots \quad (15)$$

where

$$\mu_1 = \frac{(16A_{p-n}^* - 10) - 3(5 - 4B_{p-n}^*)}{10 + 3(5 - 4B_{p-n}^*)} \quad \dots (16)$$

Thus, if we know D_{p-n} and η_{p-n} as a function of temperature and A_{p-n}^* is assumed, α_T can be calculated. A_{p-n} is known to be fairly constant (1.10) over a long range of temperature, [Saxena, 1960] and does not vary much from the nature of the potential. Further, it is shown later that α_T is insensitive to the value of A_{p-n} and so an approximate guess will serve our present purpose. In this way the form of the intermolecular potential is completely removed from the expression for α_T in favour of measureable quantities and their temperature derivatives. The only limitations of these formulae are the basic assumptions involved in the derivation of the kinetic theory of gases. The one of special interest here, rigorously speaking, is that these formulae hold only for spherically symmetric molecules. This assumption is rather serious for the case of water which is polar, but as the transport properties are less sensitive to molecular orientations and as Krieger (1951) had some success for polar molecules with an angle-independent potential, we will continue to assume the applicability of central forces.

CALCULATION OF THE THERMAL DIFFUSION FACTOR

The diffusion coefficients have been experimentally measured for the hydrogen and water system by Winkelmann (1884, 1889), Schwartz and Brow (1951) and Crider (1956). The results of Winkelmann and Crider agree with each other but are systematically lower than those of Schwartz and Brow. The reason of this disparity probably lies in the effect of supercooling at the vapour-liquid interface (Le Blanc and Wuppermann, 1916) and in the difference in the solubility of hydrogen in water. Schwartz and Brow have avoided this difficulty and I feel their data is the most reliable one at the moment. This latter data can be represented by a linear plot of $\log D$ vs. $\log T$ in the entire temperature range (307.3—352.7°K), with the average standard deviation of 0.6% only. Consequently, we will treat $(\partial \ln D / \partial \ln T)_{pr}$ as constant in the formulae of the previous section and then to this approximation, $\partial^2 \ln D / (\ln T)^2$ can be neglected in this temperature range.

The data for the viscosity of hydrogen in this temperature range is given by Trautz and Binkele (1930), Trautz and Heberling (1931), Trautz and Hussein (1934), Johnston and McCloskey (1940) and Wobser and Nuller (1941). All this data can again be represented by a linear plot of $\log \eta$ vs. $\log T$ in this temperature range with an average deviation of 0.1% only. The value of the term, $\partial \ln f_n / \partial \ln T$, was found to be negligible in this temperature range [Saxena, 1956].

Table I lists the values of the thermal diffusion factor for the two limiting ends of the composition range and for the three temperatures at which the experimental diffusion data are available. In column 2 are tabulated the α_T values, calculated according to Eq. (1) in conjunction with Eq. (6) and from (9) to (14) while the column 4 values emerge out of the use of Eqns. (15), (16) and (10). These values, designated as first set, utilise the diffusion data of Schwartz and Brow (1951) The second set of α_T values listed in columns 3 and 5 of Table I have similarly been calculated, except that the diffusion data of Winkelmann (1884, 1889) has been used. In these calculations a constant value of 1.10 for A^* was used. However, these calculations are insensitive to the A^* value, in as much as a change of 20% in A^* changes $\alpha_T(X_1 = 0, \text{ at } 328.6^\circ\text{K})$ only by 0.2%. α_T values, calculated using the diffusion data of Schwartz and Brow, are always higher than those obtained using the data of Winkelman. The author feels that the first set of α_T values is more reliable.

TABLE I
Thermal diffusion factor for $\text{H}_2\text{-H}_2\text{O}$ system

Temp. °K	α_T calculated, $X_1 = 0$		α_T calculated, $X_2 = 0$	
	First set	Second set	First set	Second set
307.3	1.21	1.04	0.812	0.61
328.6	1.24	1.07	0.812	0.61
352.7	1.30	1.08	0.812	0.61

In Table II, are tabulated the diffusion coefficients and the thermal diffusion factors at 300°K and 350°K for the various systems, permuting out of the isotopes of hydrogen (H_2 , HD and D_2) and heavy hydrogen substituted water (H_2O , HDO and D_2O). The diffusion coefficients have been calculated from the measured values for $\text{H}_2\text{-H}_2\text{O}$ system, by applying the mass correction factor. α_T values are calculated in the same way as that of Table I. The η values also were generated from the experimental values available for hydrogen and by multiplying these with appropriate mass correction factors. The α_T values for those system, where the mass ratio is considerably more than 0.1 will be somewhat inaccurate because of the use of Eq.(6). However, even for the worst case of $\text{D}_2\text{-H}_2\text{O}$, K has only a value of 0.0145 and consequently the values given in Table II can be treated as fairly reliable. These values of α_T are very useful in assessing the data obtained in connection with the enrichment of hydrogen in a thermal diffusion column, using the following chemical exchange:

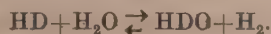


TABLE II
Diffusion coefficients and thermal diffusion factors

System	D_{T-n} in cm ² /sec.		α_T at 300°K		α_T at 350°K	
	300°K	350°K	$X_1 = 0$	$X_2 = 0$	$X_1 = 0$	$X_2 = 0$
H ₂ -H ₂ O	0.996	1.195	1.193	0.812	1.290	0.812
H ₂ -HDO	0.994	1.192	1.206	0.812	1.303	0.812
H ₂ -D ₂ O	0.991	1.189	1.217	0.813	1.316	0.813
HD-H ₂ O	0.834	1.000	1.078	0.807	1.167	0.807
HD-HDO	0.830	0.996	1.104	0.808	1.187	0.808
HD-D ₂ O	0.828	0.993	1.112	0.809	1.203	0.809
D ₂ -H ₂ O	0.739	0.886	0.970	0.803	1.052	0.803
D ₂ -HDO	0.735	0.882	0.993	0.803	1.076	0.803
D ₂ -D ₂ O	0.732	0.878	1.012	0.804	1.097	0.804

In fact, the present work was undertaken out of the need to interpret such results.

Unfortunately, at present there is no rigorous procedure for calculating the transport properties of mixtures consisting of a polar and a non-polar component. Hirschfelder, Curtiss and Bird (1954b) have advanced an approximate procedure, which also has not been extensively tested so far. This approach is based on the concept that the effective potential between a polar and a non-polar molecule has the same form as that between two non-polar molecules. An attempt is being made to assess such semi-empirical approaches proceeded by a redetermination of the force constants for pure polar gases from the upto date data.

ACKNOWLEDGMENTS

It is a pleasure to thank Dr. J. Shankar for his interest and encouragement and to Mr. P. A. Pardeshi for his help with some of the calculations.

REFERENCES

- Chapman, S. and Cowling, T. G., 1953, *The Mathematical Theory of Non-Uniform Gases*, Cambridge University Press, England.
- Crider, W. L., 1956, *J. Am. Chem. Soc.*, **78**, 924.
- Hirschfelder, J. O., Curtiss, C. F. and Bird, R. B., 1954, *Molecular Theory of Gases and Liquids*, John Wiley and Sons, Inc., New York, (a) Chapters 3 and 8; (b) p. 600-604.
- Johnston, H. L. and McCloskey, K. E., 1940, *J. Phys. Chem.*, **44**, 1038.
- Keenan, J. H. and Keyes, F. G., 1954, *Thermodynamic Properties of Steam*, John Wiley and Sons, Inc., New York.
- Kihara, T., 1949, *Imperfect Gases*, originally published in Japanese by Asakusa Bookstore, Tokyo, Japan, and translated into English by the U.S. Office of Air Research, Wright-Patterson Air Force Base. See also *Revs. Modern Phys.*, 1953, **25**, 831.

- Krieger, F. J., 1951. The Viscosity of Polar Gases, Project Rand Report RM-646.
- Lawson, A. W., Lowell, R., and Jain, A. L., 1959, *J. Chem. Phys.*, **30**, 643.
- Le Blanc, M. and Wuppermann, G., 1916. *Z. physik. Chem.*, **91**, 143.
- Liley, P. E., Thermodynamic and Transport Properties of Gases, Liquids and Solids, published by the American Society of Mechanical Engineers, New York, pages 211-219.
- Mason, E. A., 1957, *J. Chem. Phys.*, **27**, 75, 782.
- Pierce, R. W., 1959. Doctoral Dissertation, Columbia University, New York, U.S.A.
- Powel, P. E., 1958, *Advanced in Phys.*, **7**, 276.
- Saxena, S. C., 1956, *J. Phys., Soc. Japan.*, **11**, 367.
- Saxena, S. C., 1960, To be published in *Physica*.
- Schwartz, F. A. and Brow, J. E., 1951, *J. Chem. Phys.*, **19**, 640.
- Trautz, M. and Binkele, H. E., 1930, *Ann. Physik.*, **5**, 561.
- Trautz, M. and Heberling, R., 1931, *Ann. Physik.*, **10**, 155.
- Trautz, M. and Husseni, I., 1943, *Ann. Physik.*, **20**, 121.
- Weissman, S. Saxena, S. C., and Mason, E. A., 1960, *Phys. Fluids*, July-August issue.
- Winkelmann, A., 1884, *Wied. Ann.*, **22**, 152.
- Winkelmann, A., 1889, *Wied. Ann.*, **36**, 93.
- Wobser, R., and Muller, F., 1941, *Kolloid-Beih.*, **52**, 165.

A NOTE ON HEAT TRANSFER AND FILM BOILING

R. D. RAO, H. S. DESAI AND D. V. GOGATE

PHYSICS DEPARTMENT, M. S. UNIVERSITY, BARODA

(Received May 31, 1960)

ABSTRACT. Heat transfer between electrically heated metal wires and different boiling liquids has been studied and characteristic boiling curves are obtained by plotting the heat flux q/A against the excess of temperature Δt of the wire over the boiling point. The relation between the heat transfer coefficient h and Δt has also been studied. The values of maximum heat flux and critical temperature difference are calculated for the different wires and liquids used in this investigation.

INTRODUCTION

It is a matter of common experience that when a red hot metal is quenched in water, the metal first cools slowly, then rapidly and then slowly again. This can be taken as a good illustration of the three possible types of boiling, viz.—film boiling, nucleate boiling and natural convection boiling. Film boiling is that type of boiling which occurs when a vapour film exists between a heated surface and a boiling liquid. In nucleate boiling, vapour bubbles originate from different parts of the heated surface. Natural convection boiling takes place when the difference of temperature between the heated surface and the liquid is small. In the operations of jets and rockets, there are frequent contacts between a boiling liquid and a hot surface and this is the condition for film boiling. In an electrically heated boiler or an atomic power plant where the heat input is the controlled variable, there is always a danger that the temperature of the heated object may rise abruptly if the heat input is near the critical heat flux (q/A). This danger becomes much more pronounced if the value of the heat input is above the maximum heat flux $(q/A)_{max}$. If the abrupt temperature rise is sufficiently large, it may give rise to sudden expansion and weakening of certain parts of the system, sometimes causing breakage.

In view of the above importance of film boiling and nucleate boiling, we have tried (1) to investigate the effect of quenching electrically heated wires in different liquids and (2) to study the heat transfer, by means of characteristic boiling curves (incorporating free convection boiling, nucleate boiling and film boiling) between cylindrical metal wires and boiling liquids.

Drew and Mueller (1937) and others have studied heat transfer to boiling liquids by steam condensing method. Nukiyama (1934) succeeded in obtaining almost complete boiling curves by electrically heating thin platinum wires submerged

in boiling water. Natural convection boiling and nucleate boiling of water for different pressures have been studied by Addoms (1948) using thin platinum wires. Extensive study of film boiling was made by Bromley (1950) using various organic liquids.

During our study of heat transfer, we have obtained characteristic boiling curves for a number of liquids and the results of our experiments on heat transfer between cylindrical metal wires and boiling liquids have been described in this note. The complete boiling curves [plots of $\log(q/A)$ against $\log \Delta t$] for the various liquids used have been obtained for different wires, and the maximum heat flux and the critical temperature difference have been calculated. The heat flux (q/A) for unit difference of temperature between the wire and the surrounding liquid is known as the heat transfer coefficient h . Thus $h = \frac{q}{A \cdot \Delta t}$. The relation between this coefficient h and the temperature difference Δt has also been studied for liquids such as water, carbon tetrachloride, turpentine, etc. and some typical results have been graphically illustrated (Fig. 2.).

EXPERIMENTAL

The experimental arrangement consisted of a simple Wheatstone bridge with ratio arms of 1000 ohms each. A thin platinum wire which was submerged in the boiling liquid was included in the third arm of the bridge in series with an ammeter, while a small rheostat and a Eureka wire bridge with a sliding contact formed the fourth arm of the bridge.

The platinum wire was allowed to remain in the boiling liquid for some time before passing a current through it so that it attained the temperature of the boiling liquid. The resistance of the wire could then be calculated at this temperature, if R_0 , the resistance of the wire at 0°C and α , the temperature coefficient of resistance for the wire are known. A very small current which does not heat the wire appreciably, was then passed through the wire and a balance was obtained by adjusting the rheostat and by sliding the contact on the Eureka wire bridge. The current through the wire was then increased so as to raise its temperature. This increases the resistance of the wire, thus disturbing the balance previously obtained. The contact is now shifted so as to restore the balance. Knowing the value of this shift and also the resistance per unit length of the Eureka wire, the change in resistance ΔR of the platinum wire could be calculated. The excess of temperature of the wire above the boiling point of the liquid could then

be determined by means of the relation $\Delta t = \frac{\Delta R}{R_0 \alpha}$.

RESULTS AND DISCUSSION

The input power q is equal to $\frac{C^2 R}{J}$ where C is the current passing through the wire, R is its resistance and J is the mechanical equivalent of heat, The heat

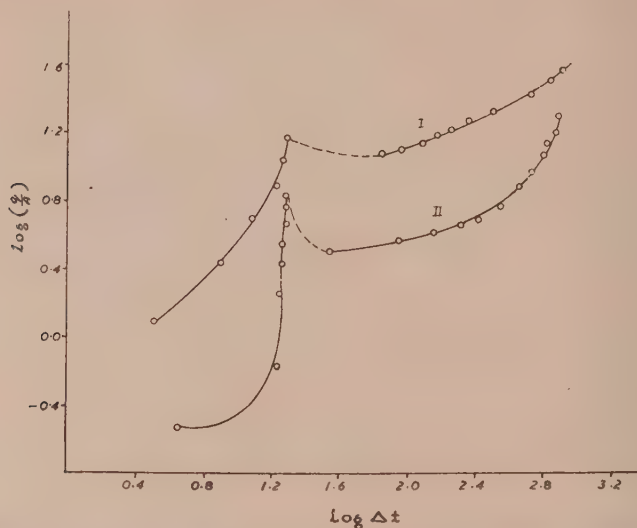


Fig. 1. Curves showing the variation of q/A with the excess of temperature.
Curve I—Platinum-water. Curve II—Platinum-carbontetrachloride.

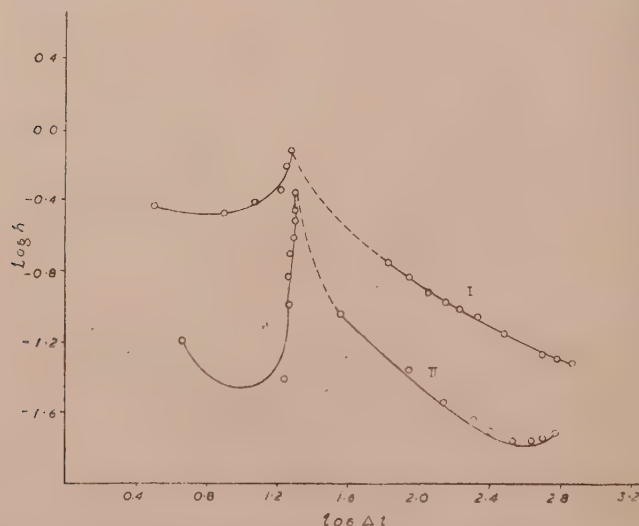


Fig. 2. Curves showing the variation of h with the excess of temperature.
Curve I—Platinum-water. Curve II—Platinum-carbontetrachloride.

flux is given by q/A where A is the surface area $2\pi rl$ of the wire of length l and radius r . Typical curves showing the variation of q/A with the excess of temperature Δt as also the relation between the heat transfer coefficient h ($= \frac{q}{A \Delta t}$) and Δt for water and carbon-tetrachloride are exhibited in Figs. (1) and (2) respectively.

The values of the maximum heat flux $(q/A)_{max}$ and critical temperature difference Δt_{crit} for the different wires and liquids used as also the values of the slopes calculated for natural convection boiling and nucleate boiling together with the heat transfer coefficient (h) at the peak value are shown in Table I.

TABLE I

Liquid	Wire	Slopes for		$\left(\frac{q}{A}\right)_{max}$ cal/sec. cm ²	Δt_{crit}	$(h)_{max}$ cal/cm. ² sec°C
		Nat. conv. boiling	Nucl. boiling			
Water (B.P. 100°C)	Platinum	0.91	3.25	15.8	19°C	0.800
Turpentine (B.P. 166°C)	-do- $r = 0.005$ cm.	1.2	3.6	12.02	39.8°C	0.302
	Copper $r = 0.0026$ cm.	1.0	4.66	10.96	36.3°C	0.302
	Tungsten $r = 0.0028$ cm.	0.9	1.6	12.6	43.6°C	0.275
Naphthalene (B.P. 215°C)	Platinum	0.77	2.8	11.48	39.8°C	0.288
	Copper	0.83	2.75	10.72	39.8°C	0.263
	Tungsten	1.0	1.7	12.59	38.02°C	0.331
Carbontetrachloride (B.P. 77°C)	Platinum	0.6	2.57	6.9	19.95°C	0.355
	Tungsten	0.71	3.0	8.7	22.9°C	0.355

When the heat flux exceeds $(q/A)_{max}$ the system passes from nucleate boiling regime to film boiling regime after passing through a transient state of unstable film boiling. This unstable (transient) state is shown by the dotted curve in Figs. (1) and (2). In the state of stable film boiling a vapour film is formed between the wire and the liquid. This film acts as a barrier in which the heat flow is due more to conduction than to convection. The formation of this barrier (vapour blanket) naturally diminishes the heat flow from the wire to the liquid and hence the value of heat transfer coefficient h is also decreased as indicated by the graphs in Fig. 2. These graphs also indicate that if the heat flux is still further increased, the value of h goes on decreasing further.

CONCLUSIONS

(a) The material and dimensions of the wire do not seem to affect the value of the maximum heat flux $(q/A)_{max}$ so much as the properties of the liquid, especially the latent heat of vaporisation.

(b) The continued decrease in the value of h with the increase of heat flux in the film boiling regime seems to be due to a slight increase in the thickness of the vapour film.

REFERENCES

- Addoms J. N., 1948, "Heat Transmission" by William H. McAdams, McGraw-Hill Third Edition 1954 page 382 in Asian students' Edition.
- Bromley, L. A., 1950, *Chem. Eng. Progr.*, **46**, 221.
- Drew, T. B. and Mueller, A. C., 1937, *Trans. Am. Inst. Chem. Engrs.*, **33**, 449.
- Nukiyama, S., 1934, *J. Soc. Mech. Engrs.*, (Japan), **37**, 367., 853-54.

THE DIELECTRIC PROPERTIES OF COPAL ESTER

A. K. SEN and G. N. BHATTACHARYA

DEPARTMENT OF APPLIED PHYSICS, CALCUTTA UNIVERSITY

(Received, July 27, 1960)

ABSTRACT. The dielectric properties of copal ester have been measured over a wide range of temperature and frequency viz., from 25°C to 160°C and from 400 c/s to 300 kc/s. Within the temperature range of investigation copal ester behaves as a typical polar resin in the anomalous dispersion range. The loss curves have unusually broad peaks which suggest a highly distributed relaxation time of its orientating polar units. This is corroborated from the shape of the ϵ''/ϵ_m'' vs $\log f/f_m$ curve as well as a high value of the distribution factor calculated from the Cole and Cole diagram. With the help of melt viscosity data of this resin the size of its rotating unit has been calculated following Debye's relation and the calculated radius comes out to be about 1.5 Å, which is the same as that of a hydroxyl group. The presence of the hydroxyl group is clearly indicated in the infrared absorption spectrum of this resin, which suggests these groups to be its actual rotating units.

INTRODUCTION

Copals are a general name for various fossil and semi-fossil resins found in some tropical countries. They are usually named after their places of origin. Like rosin, copals have a high acid value and they differ somewhat in their chemical and physical properties depending upon their composition. Copal esters, however, are important as they are widely used in the preparation of insulating varnishes, impregnating compounds, moulded insulation etc.

Bhattacharya (1946) studied the dielectric properties of Marila Copal, while Clare (1949) reported the dielectric properties of Kauri copal. But recently the application of Debye's equation for obtaining the size of the rotating unit in a few natural resins has revealed some interesting fact. In the case of rosin (Sen and Bhattacharya, 1958a) the radius obtained is equal to the effective radius of abietic acid molecule, the chief constituent of rosin, whereas in the case of ester gum (Sen and Bhattacharya, 1958b) which has a much bigger molecule, a similar calculation yields a much smaller value for the radius, viz., that of the hydroxyl group. The fact that ester gum contains hydroxyl group has been corroborated later from the infrared absorption curve.

It was concluded, therefore, that perhaps the unesterified hydroxyl groups of mono- and di-abietates in ester gum were the actual rotating units. If now mono- and di-abietates are formed during the esterification of rosin, it is natural to expect

a similar formation of mono- and di-glycerides during the esterification of similar other resins with glycerol. If in these esters too the value of the radius comes out to be that of the hydroxyl group our conclusions regarding the rotating unit in ester gum can be justified to some extent. With this end in view the measurement of the dielectric properties of the glycerol esters of copal has been undertaken.

THEORETICAL AND EXPERIMENTAL

The theoretical aspects of dielectric measurement have been fully discussed before (Sen and Bhattacharya, 1958a and 1958b) and the procedure for the measurement of permittivity, power factor, resistivity and viscosity are the same as reported earlier (Sen and Bhattacharya, 1957, 1958a & b).

Infrared absorption curves

(1) *Recording of absorption curves*

Absorption measurements were done on a Hilger infrared spectrophotometer, model H 800, using a rock-salt prism as the dispersion element in the range of 1 to 15 microns. The instrument was used in the double beam position, where the transmission through the test medium was automatically balanced with the transmission through air. A Brown-Electronik recording potentiometer was used for obtaining the absorption-wavelength curve. This curve was photographically reduced to convenient size.

(2) *Preparation of test-pieces.*

Wires of 28 S.W.G. were made into rectangular frames of dimensions approximately $1'' \times \frac{1}{2}''$. Films were formed on the wire frames from molten resin having appropriate viscosity and surface tension depending upon temperature. Sufficient care was taken in preparing the films of required thickness making a compromise between maximum transmission and mechanical stability.

DISCUSSION

The results of measurement of dielectric constant ϵ' , dielectric loss ϵ'' , and power factor $\tan \delta$ for various temperatures and frequencies are shown graphically in Figs. 1, 2, and 3 respectively.

These curves also indicate the characteristics of a typical polar substance in the anomalous dispersion range. The power factor as well as the dielectric loss curves begin to rise from about 50°C. The loss maxima for 10 kc/s, 50 kc/s, 100 kc/s and 300 kc/s are more or less of the same value and it is about 0.09 while for 400 c/s and 1 kc/s they are slightly higher. The range of temperature over which the different peaks are distributed is about 42°C.

The striking feature of these loss curves is their unusually broad peaks. The dielectric constant curves are also flat. The nature of these curves indicates

the effects of distributed relaxation time in a greater degree. From Fig. 4 it may also be seen that the region of dispersion spreads over at least 5 to 6 decades

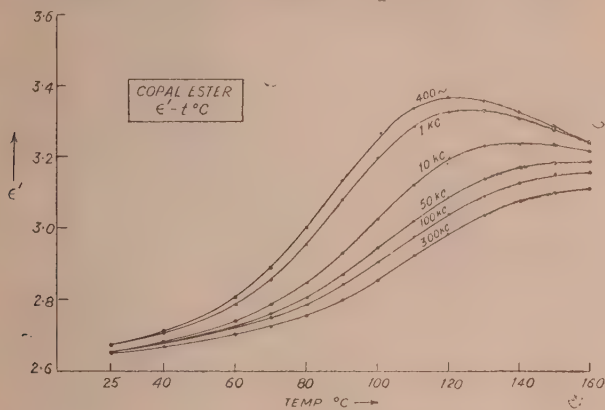


Fig. 1

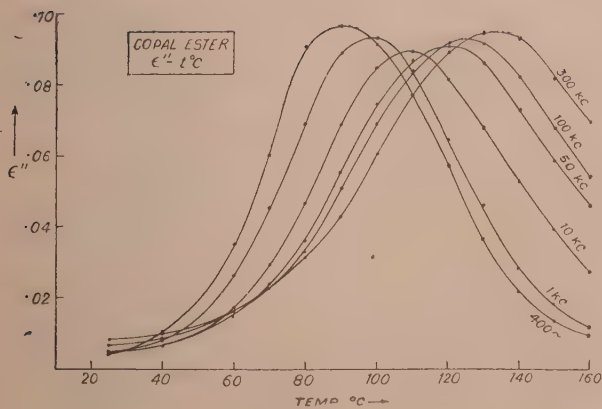


Fig. 2.

of frequency. The Cole and Cole diagram for this resin is shown in Fig. 6. Although the experimental curve is a circular arc its centre lies considerably below the abscissa signifying a wide distribution of relaxation times. The value of the distribution factor h calculated from the diagram is 0.69 compared to 0.52 for ester gum. The ϵ''/ϵ''_m vs $\log f/f_m$ curve in Fig. 7 also reveals this high degree of distribution.

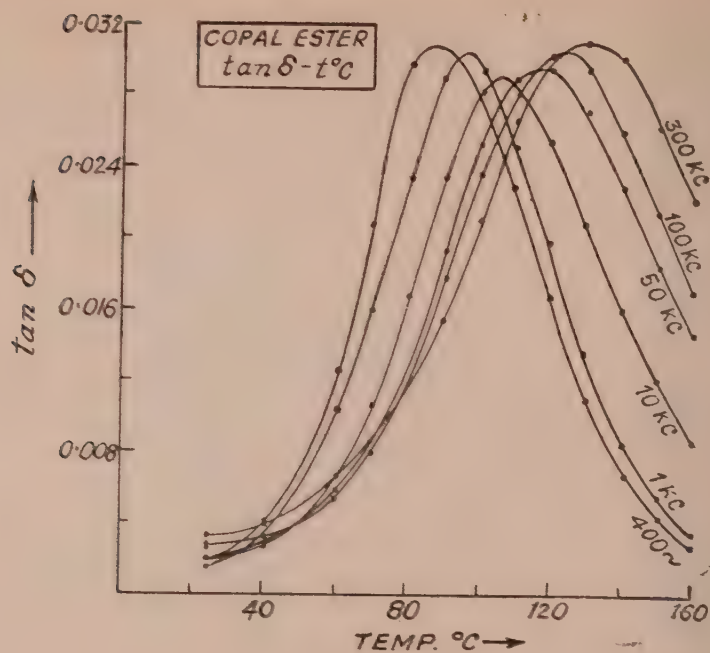


Fig. 3.

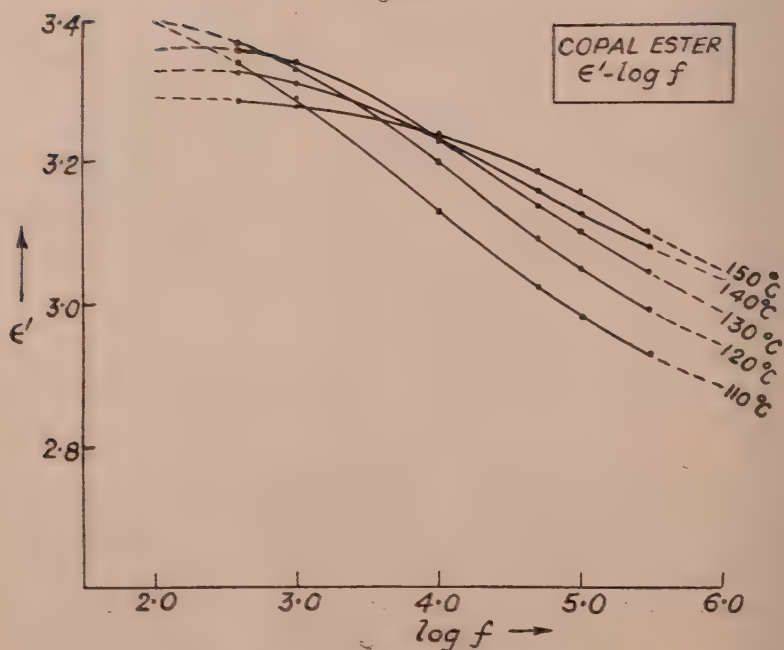


Fig. 4.

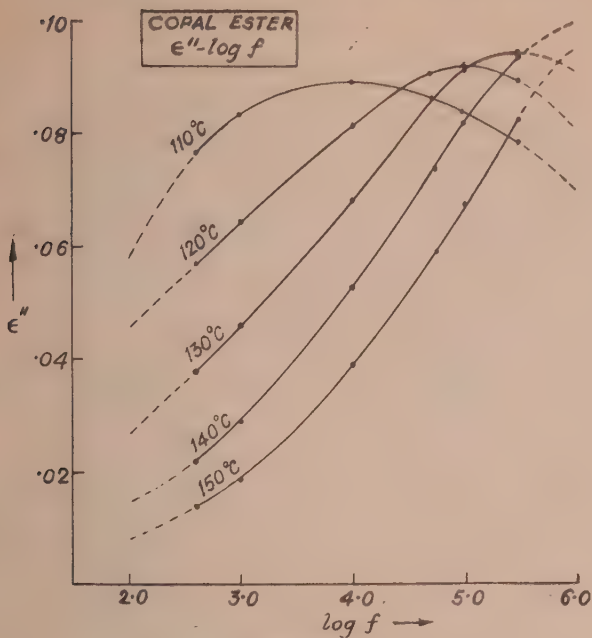


Fig. 5.

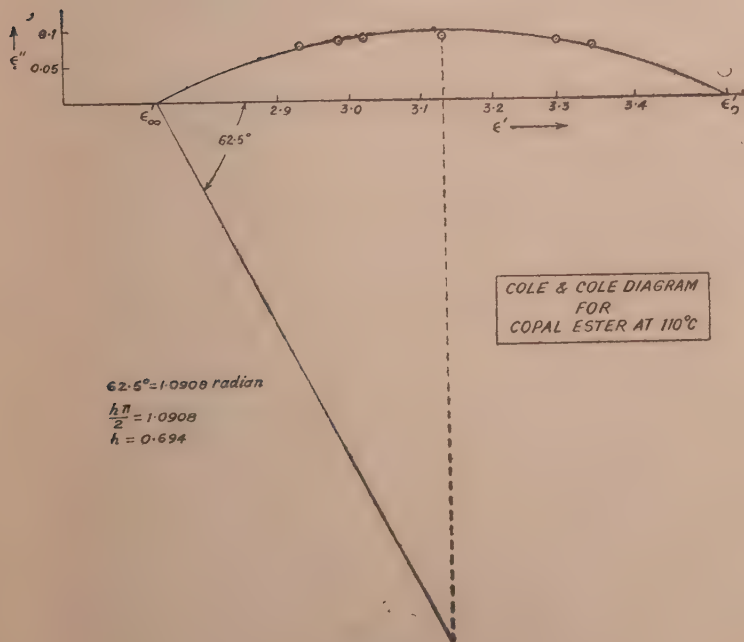


Fig. 6.

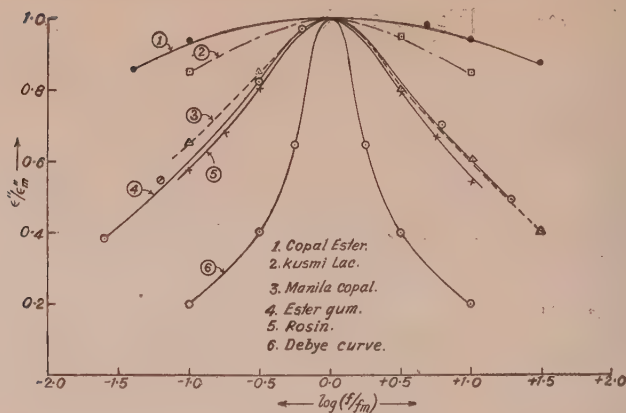


Fig. 7.

We may now calculate the value of the radius of the rotating unit in this resin from the relaxation time at the temperature of a loss-maximum and its melt viscosity at that temperature.

The melt viscosity of copal ester was determined in the same way as in the case of other resins. The results are shown in Table I and the graph of $\log \eta$ against $1/T$ is shown in Fig. 8.

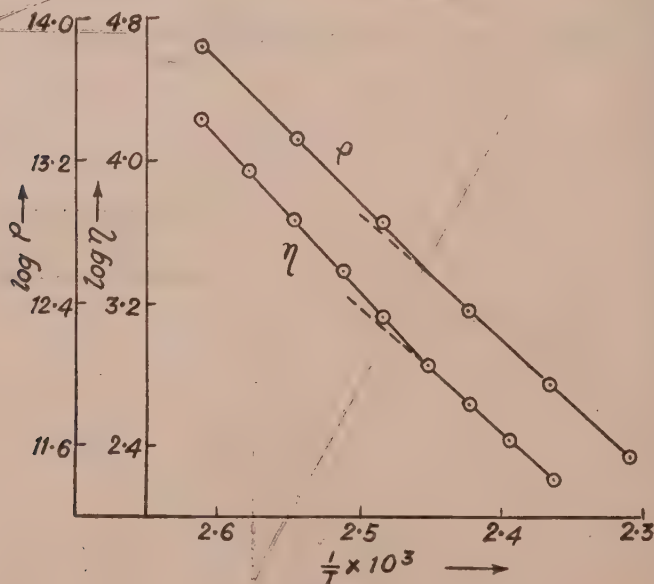


Fig. 8.

TABLE I
Viscosity—temperature data

Temperature		$\frac{1}{T} \times 10^3$	Viscosity η in poise	$\log \eta$
$t^\circ\text{C}$	$T^\circ\text{K}$			
110	383	2.611	16,630	4.2208
115	388	2.577	8,710	3.9400
120	393	2.545	4,480	3.6513
125	398	2.513	2,400	3.3802
130	403	2.481	1,320	3.1205
135	408	2.451	680	2.8325
140	413	2.421	420	2.6232
145	418	2.392	260	2.4150
150	423	2.364	160	2.2041

For comparing the internal friction involved in viscosity and resistivity, the curve of $\log \rho$ plotted against $1/T$ is incorporated in the same figure. Resistivity and conductivity data are given in Table II.

TABLE II
D.C. conductivity or resistivity—temperature data

Temperature		$\frac{1}{T} \times 10^3$	Conductivity k in mho cm^{-1}	Resistivity ρ in ohm cm	$\log \rho$
$t^\circ\text{C}$	$T^\circ\text{K}$				
110	383	2.611	0.152×10^{-13}	6.575×10^{13}	13.8179
120	393	2.545	0.475×10^{-13}	2.104×10^{13}	13.3231
130	403	2.481	0.146×10^{-12}	6.837×10^{12}	12.8349
140	413	2.421	0.437×10^{-12}	2.289×10^{12}	12.3595
150	423	2.364	0.112×10^{-11}	8.940×10^{11}	11.9513
160	433	2.309	0.284×10^{-11}	3.525×10^{11}	11.5471

The slopes of both the viscosity and resistivity curves are identical signifying that the same energy of activation is involved in both the processes. As in the case of ester gum (Sen and Bhattacharya, 1957) a transition point is also seen in this resin near about 130°C . The slopes of both the viscosity and resistivity curves change abruptly at this temperature in a similar way signifying some change of state at this temperature.

The radius of the rotating unit is computed using Debye's equations and the results are shown in Table III.

TABLE III
Calculated relaxation time and radius of the rotator

Frequency in kc/s	Loss maximum temperature t_m in $^{\circ}\text{C}$	Relaxation time τ in sec.	$\log \eta$ at t_m	Radius of the rotator a in \AA
10	110	1.424×10^{-5}	4.22	1.53
50	121	2.859×10^{-6}	3.60	1.45
100	127	1.434×10^{-6}	3.26	1.50
300	135	4.808×10^{-7}	2.82	1.48

The chemical composition of manila copal has been studied by various workers and according to them it consists of several acids. According to Tschirch and Koch (1902) the major constituents of manila copal (comprising about 75% of the total) are two isomeric forms of mancopalic acid, viz., α and β -mancopalic acid having the chemical formula $\text{C}_{19}\text{H}_{17}\text{COOH}$. Other constituent acids have more or less similar chemical formula. Therefore, glycerol esters of these acids should—even on a moderate estimate, be big molecules—much bigger than the values shown in Table III. Therefore, rotation of the entire molecule seems improbable in this resin also. A segment or a part of the molecule or some groups attached to it may be the actual rotator here.

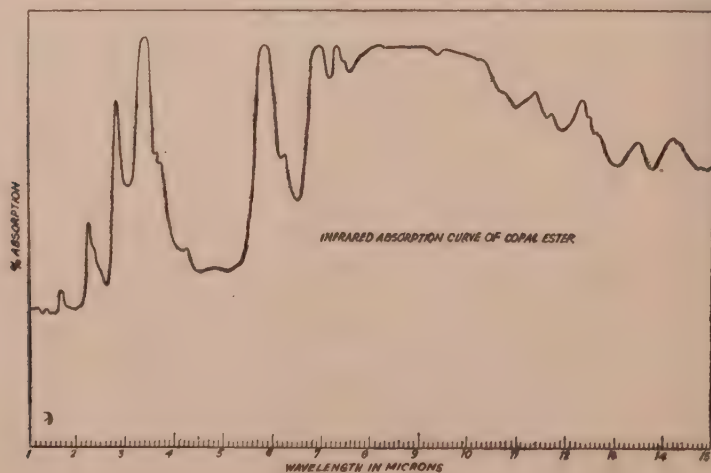


Fig. 4.

The values of the radii obtained are the same as in the case of ester gum, viz., that of a hydroxyl group. The presence of hydroxyl groups in ester gum has been conclusively proved and they can be explained as due to the presence of mono- and di-glycerides formed during the esterification of rosin with glycerol. In copal ester also the presence of hydroxyl groups can be similarly expected. But this view can be justified if their presence can be similarly demonstrated on the basis of other evidences.

From the infrared absorption curve shown in Fig. 9 it may be seen that an absorption peak occurs at the wavelength of 2.78μ signifying the presence of hydroxyl groups also in this resin as in the case of ester gum.

ACKNOWLEDGMENTS

The authors are grateful to the Director, Central Glass and Ceramics Research Institute, Calcutta, under the Council of Scientific and Industrial Research Government of India, for providing them with the facilities available there for obtaining the infrared absorption spectrogram of this resin. They also wish to express their thanks to Messrs. Jenson and Nicholson (India) Ltd. for the supply of a sample of copal ester.

REFERENCES

- Bhattacharya, G. N., 1946, *J. Sc. & Ind. Res.*, **4B**, 713.
Clare I. C., 1949, *Elastomers and Plastomers* (Elsevier Publishing Co., New York), **2**, 371.
Sen, A. K. and Bhattacharya, G. N., 1957, *J. Assoc. App. Physicists.*, **4**, 72.
Sen A.K. and Bhattacharya G. N., 1958a, *Ind. J. Phys.*, **32**, 556.
Sen A. K. and Bhattacharya, G. N., 1958b, *Ind. J. Phys.*, **32**, 49.
Tschirch and Koch, 1902, *Arch. Pharm.*, **240**, 202.

THE LIFETIME OF HYPERFRAGMENTS*

G. C. DEKA

DEPARTMENT OF PHYSICS, COTTON COLLEGE, GAUHATI

(Received, May 19, 1960)

ABSTRACT. Available data on the time of flight of hyperfragments have been used to deduce a lifetime for light hypernuclei, and the value thus obtained is discussed.

During recent years a large number of nuclear fragments, so-called hyperfragments (HF) which contain a Λ^0 hyperon have been observed in nuclear emulsions and their proper analysis has also been made. Along with other properties the Λ^0 hyperon binding energy of most of the low charged ($Z \leq 3$) HFs have been measured. An extensive search on the subject was also made by the author (Thesis 1959), and the results have been published in *Nuovo Cimento* (1959). A detailed survey of the available data was reported by Levi-Setti *et al.* (1958). An interesting aspect of the subject which is not yet attempted by any previous worker is the measurement of the lifetime of such HFs and a comparison with that of a free Λ^0 hyperon decay. The latter is however fairly well known from different chamber experiments. Several authors using statistical procedures have estimated the mean lifetime of the free Λ^0 particle. A value reported by Blumenfeld *et al.* (1956) is $2.8 \pm .4 \cdot 10^{-10}$ sec obtained on the basis of 65 events observed in a 36" multiplate cloud chamber exposed to a π -meson beam at Brookhaven. A recent value quoted by Raman (1960) in his book is $2.6 \pm .16 \cdot 10^{-10}$ sec which includes data upto 1959.

When measuring the lifetime of HFs there are a number of experimental difficulties e.g.

- i) Most of the HFs decay at rest permitting thereby only the measure of moderation time which is a lower estimate of the mean life.
- ii) Decays in flight which yield information about the mean life are difficult to detect and identify due to the similar events recorded in emulsions.
- iii) Non mesonic decays are very often missed in observations.
- iv) Heavy HFs, which are usually short evaporation tracks, cannot be identified nor their velocity at production can be calculated.

The experiments made and the procedures adopted by the author are briefly as follows :

*The preliminary result of this paper was reported in the Cosmic Ray symposium held at Ahmedabad, 1960.

A stack of Ilford G5 emulsions exposed to an intense beam of 4.5 BeV π^- mesons from Berkeley Bevatron was area scanned under low magnification. All double stars which may be possible HFs were picked up. Another stack of K5 emulsions exposed to a beam of 300 MeV c K^- -mesons from the same machine was line scanned for double stars. All the secondary particles emitted from the second stars were followed to their ends, and their energy and momentum were determined from the observed ranges.

Out of 51,000 pion interactions 98 double stars and of 1300 K^- -interactions at rest 61 double stars were picked up and analysed by applying a few selection criteria in order to minimise the bias, arising out of similar events like nuclear collisions, captures of negatively charged particles and chance coincidences.

The interconnecting track of every star was closely examined for its multiple scatterings and the thinning down near the second star, the features which usually indicate the stopping of a particle. For a flat interconnector of range $\geq 20\mu$ it may be possible to exclude π^- meson-capture, as the high multiple scatterings of such a track is distinctive. In a very few cases the charge Z of the HF could also be determined from δ -ray observation or by profile measurements on the tracks. The non mesonic decays in flight of heavy HFs were indicated by the presence of δ -rays closed to the second star. Sometimes the mass of a long ranged HF can be determined from multiple scatterings by a constant sagitta method. To define a HF decay the information from the detailed analysis of the second star was taken. A HF which decays into two charged particles producing two collinear tracks or, into three charged particles producing three co-planar tracks could be uniquely defined. Others, for which are obtained a sensible Λ -binding energy when the unbalanced momentum is given to one neutron only, are also considered to be nearly unique. Besides, there are a number of events which

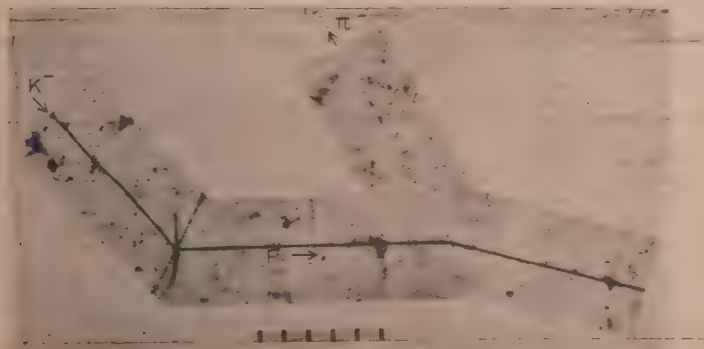


Fig. 1. H^4 -hypernucleus ejected from a K^- -capture star, decaying in flight into $H_e^4 + \pi^-$.

cannot be interpreted from such analysis, but may not show any feature which can exclude them from being HF decay.

The time of flight or the moderation time of the well defined HF's are determined from their observed range by using the recent range-energy relations given by Barkas (1957).

Two HF decays in flight have been reproduced in Figs. 1 and 2.

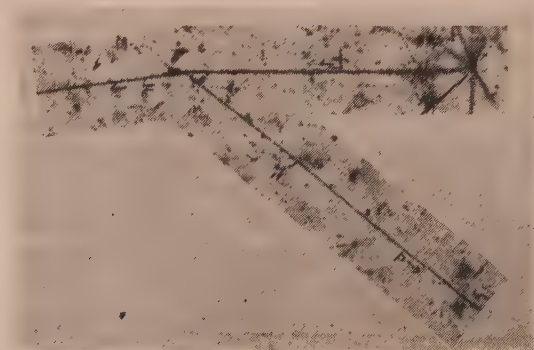


Fig. 2. $B^{10}_{\pi^{11}}$ —hypernucleus ejected from a 4.5 BeN π^- meson decaying in flight into $He^4 + p + n$ (2).

The available data has been listed in the Tables I and II

TABLE I
Events observed by the author

	HF's	No. of events observed		Total time of flight in 10^{-10} sec.
		At rest	In flight	
Mesonic decays	He^4	4	1	0.64
	He^4	4		0.07
	He^5	6		1.50
	Li^7	1		0.04
	Be^8	1		0.07
Non-mesonic decays	He^4	1		0.08
	$Li^6_{\pi^7}$...	1	0.18
	$B^{10}_{\pi^{11}}$...	1	0.03

TABLE II
Events observed by other authors

	HFs	Time of flight in 10^{-10} sec.	Reference
Mesonic decays	H ³ (f)	1.30	Friedlander <i>et al.</i> , 1956.
	H ³ („)	0.06	Filipkiwski, <i>et al.</i> , 1958.
	H ⁴ „	0.22	-do-
	He ⁴ „	0.77	Fowler and Hansen, 1956.
	H ³ „	1.10	Cloud Chamber expt.
	He ⁴ „	5.00	-do-
	H ³ „	0.02	Sorensen, <i>et al.</i> , 1956.
	He ⁴ „	5.40	Sorrel, <i>et al.</i> , 1955.
	H ³ (r)	1.30	Castagnoli, <i>et al.</i> , 1955.
	H ³ „	0.45	Herman Yagoda, 1955.
	H ³ „	0.15	Imaeda, <i>et al.</i> , 1958.
	H ³ „	0.15	-do-
	H ³ „	0.22	-do-
	He ⁵ „	0.50	Hill, <i>et al.</i> , 1956.
	Li ⁷ „	1.00	Filipkowski, <i>et al.</i> , 1956.
Non-mesonic decays	H ⁴ (f)	0.11	Fry, <i>et al.</i> , 1958.
	Be (r)	0.11	Castagnoli, <i>et al.</i> , 1955.
	B „	0.76	-do-

Ignoring the biases against detecting decays in flight and the non mesonic decays, a life time has been deduced from the above data. Such values are the following :

(1) $2.7 \pm 0.9 \times 10^{-10}$ sec for the mesonic decay,

(2) $0.4 \pm 0.2 \times 10^{-10}$ sec for the non-mesonic decay.

This shows that there is little difference between the lifetime for HFs decaying mesonically and that for a free Λ^0 decay. The much lower value for the non-mesonic decay is apparently due to the considerably fewer events.

It is however to remark that as the experimental materials may contain bias and the events cannot be selected in controlled conditions the above results cannot therefore be given an unambiguous physical interpretation. It is more an indication of the interest to collect data in a well controlled unbiased manner.

ACKNOWLEDGMENTS

The author expresses his gratitude to Prof. C. F. Powell F.R.S. for his hospitality and the use of the facilities of the H. H. Wills Physical Laboratory, Bristol where the experimental work included in this paper was done. He also likes to thank Dr. D. Evans of Bristol for his helpful suggestions. He thanks the Govt. of Assam for providing facilities for such a piece of research work in Cotton College, Gauhati.

REFERENCES

- Bluenfield, H., Chonowsky, W. and Lederman, L. N., 1958, *Il Nuovo Cim.*, **2**, 296.
Barkas, W. H., Report UCRL 2426, Rev. 1957.
Deka, G. C., 1959, *Il. Nuovo Cim.*, **6**, 1217.
Filipkowski, A. and Skrazypczar. E., 1956, Pol. Akadami Report no. 24/vi.
Filipkowski, A., Gierula, J. and Zielinski, P., 1957, *Acta. Phys. Polon.*, **16**, 159.
Levi Setti, R., Slater, W. E., and Telegdi, V. L., 1958, *Il. Nuovo Cim. Suppl.*, **1**, 10.
Raman, P., 1960, "The theory of elementary particles".

IMPEDANCE MATCHING BY RE-ENTRANT STUB LINE

G. S. SANYAL

INDIAN INSTITUTE OF TECHNOLOGY, KHARAGPUR

(Received, August 23, 1960)

ABSTRACT. This article describes a new method of matching a load to a transmission line. This is suitable for narrow band matching when the load V.S.W.R. is greater than 4.

INTRODUCTION

It is well known that for efficient transfer of power and for other considerations, a transmission line is required to be matched to the load. In many cases, however, the load presents an impedance different from the characteristic impedance of the transmission line necessitating some device to match the load to the line. At frequencies where lumped networks are not suitable, the devices normally employed for narrow band matching are stub lines, quarter-wave transformers, or dielectric sleeves. To these may be added a re-entrant stub line matching section as shown in Fig. 1.

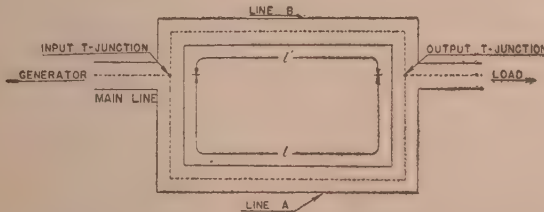


Fig. 1. Re-entrant stub line matching section using coaxial line.

Two transmission lines A and B are connected in parallel to form a re-entrant double stub line. It will be shown that if the two line lengths l and l' are appropriately selected the impedance at the output T -junction is transformed to the desired value at the input junction. The range of impedances at the output T -junction that can be matched to the input line depends upon the characteristic impedances of lines A and B relative to the main line. Theoretically, by proper choice of the characteristic impedances of lines A and B , it is possible to make the main line flat for any load V.S.W.R. at the output junction. In practice, however, the case of importance will be when the characteristic impedance of *all* the lines are identical. Only this case will, therefore, be considered. This consideration restricts the use of the re-entrant stub line section as a matching device to load V.S.W.R. equal to or higher than 4. The analysis together with some experimental results are presented in this article.

MATRIX PARAMETERS OF TRANSMISSION LINES

The input and output currents I_1 and I_2 of a uniform, loss-less transmission line of length l shown in Fig. 2(a) can be expressed in terms of the corresponding voltages E_1 and E_2 by

$$\left. \begin{aligned} I_1 &= -j Y_0 (\cot \beta l) E_1 + j Y_0 (\operatorname{cosec} \beta l) E_2 \\ I_2 &= j Y_0 (\operatorname{cosec} \beta l) E_1 - j Y_0 (\cot \beta l) E_2 \end{aligned} \right\} \quad \dots (1)$$

where Y_0 and β ($= 2\pi/\lambda$) are the characteristic admittance and the phase constant respectively of the line and λ is the wavelength.

In matrix notation Equ. (1) is written as

$$\begin{bmatrix} I_1 \\ I_2 \end{bmatrix} = \begin{bmatrix} -j Y_0 \cot \beta l & j Y_0 \operatorname{cosec} \beta l \\ j Y_0 \operatorname{cosec} \beta l & -j Y_0 \cot \beta l \end{bmatrix} \times \begin{bmatrix} E_1 \\ E_2 \end{bmatrix} \quad \dots (2)$$

$$\text{i.e.,} \quad [I] = [Y] \times [E]$$

We can, therefore, represent a given length of transmission line by a two-terminal pair network, shown in Fig. 2(b), provided their admittance matrices

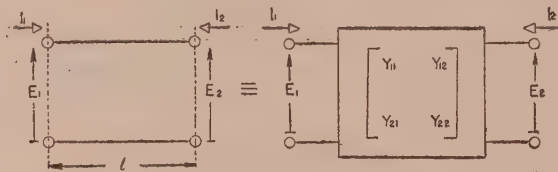


Fig. 2(a). Loss-less transmission line of length l and characteristic admittance Y_0 .

Fig. 2(b). Equivalent network representation of the transmission line.

are identical. For the equivalent network the elements of the admittance are obtained from

$$[Y] = j Y_0 \begin{bmatrix} -\cot \beta l & \operatorname{cosec} \beta l \\ \operatorname{cosec} \beta l & -\cot \beta l \end{bmatrix} \equiv \begin{bmatrix} Y_{11} & Y_{12} \\ Y_{21} & Y_{22} \end{bmatrix}$$

$$\text{i.e.,} \quad \left. \begin{aligned} Y_{11} &= Y_{22} = -j Y_0 \cot \beta l \\ Y_{12} &= Y_{21} = j Y_0 \operatorname{cosec} \beta l \end{aligned} \right\} \quad \dots (3)$$

Let us now consider the two lines A and B , one (A) of length l and the other (B) of length l' , each of characteristic admittance Y_0 connected as shown in Fig. 1. The equivalent network representation is shown in Fig. 3 where the unprimed quantities refer to line A and the primed quantities to line B .

The resultant $[Y]$ matrix of the parallel combination of the two networks is thus from Equ. (3).

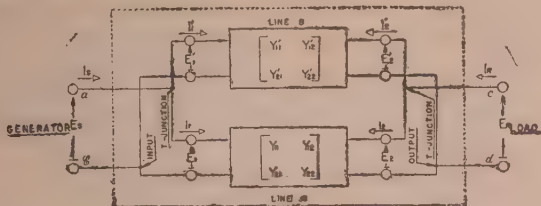


Fig. 3. Equivalent network representation of the re-entrant stub line.

$$\begin{aligned} \text{Resultant } [Y] &= \begin{bmatrix} Y_{11} + Y'_{11} & Y_{12} + Y'_{12} \\ Y_{21} + Y'_{21} & Y_{22} + Y'_{22} \end{bmatrix} \\ &\equiv jY_0 \begin{bmatrix} -(\cot \beta l + \cot \beta l') & (\operatorname{cosec} \beta l + \operatorname{cosec} \beta l') \\ (\operatorname{cosec} \beta l + \operatorname{cosec} \beta l') & -(\cot \beta l + \cot \beta l') \end{bmatrix} \quad \dots (4) \end{aligned}$$

The matrix representation (4) now leads us to a single equivalent network of the re-entrant stub line section as far as the input (terminals $a-b$) and output (terminals $c-d$) are concerned. This is shown in Fig. 4.

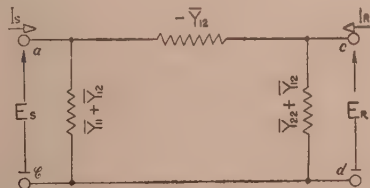


Fig. 4. Resultant network configuration of the re-entrant stub line.

In the above representation,

$$\left. \begin{aligned} \bar{Y}_{11} &= Y_{11} + Y'_{11} = \bar{Y}_{22} = Y_{22} + Y'_{22} \\ &= -jY_0(\cot \beta l + \cot \beta l'); \\ \bar{Y}_{12} &= (Y_{12} + Y'_{12}) = (Y_{21} + Y'_{21}) \\ &= jY_0(\operatorname{cosec} \beta l + \operatorname{cosec} \beta l') \end{aligned} \right\} \quad \dots (5)$$

If the value of the load admittance at $c-d$ is $\bar{Y}_R = -(I_R/E_R)$, it is easy to show that the input admittance at $a-b$ looking into the terminals is

$$Y_{in} = \bar{Y}_{11} - [\bar{Y}_{12}^2 / (\bar{Y}_{22} + Y_R)] \quad \dots (6)$$

IMPEDANCE MATCHING

We now propose to show that for Y_R lying within a certain range defined later, it is possible to make $Y_{in} = Y_0$ by appropriate choice of the lengths of the lines A and B . The condition required for matching is $Y_{in} = Y_0 + j(0)$. The desired line lengths $\theta (= \beta l)$ and $\theta' (= \beta l')$ are then obtained from Eq (5) and (6) and are governed by the following two simultaneous equations :

$$\left. \begin{aligned} g_R(\operatorname{cosec} \theta + \operatorname{cosec} \theta')^2 &= g_R^2 + (b_R + \cot \theta + \cot \theta')^2 \\ \frac{(b_R + \cot \theta + \cot \theta')(\operatorname{cosec} \theta + \operatorname{cosec} \theta')^2}{g_R^2 + (b_R + \cot \theta + \cot \theta')^2} &= \cot \theta + \cot \theta' \end{aligned} \right\} \dots (7)$$

where

$$g_R - jb_R = Y_R/Y_0 = y_R.$$

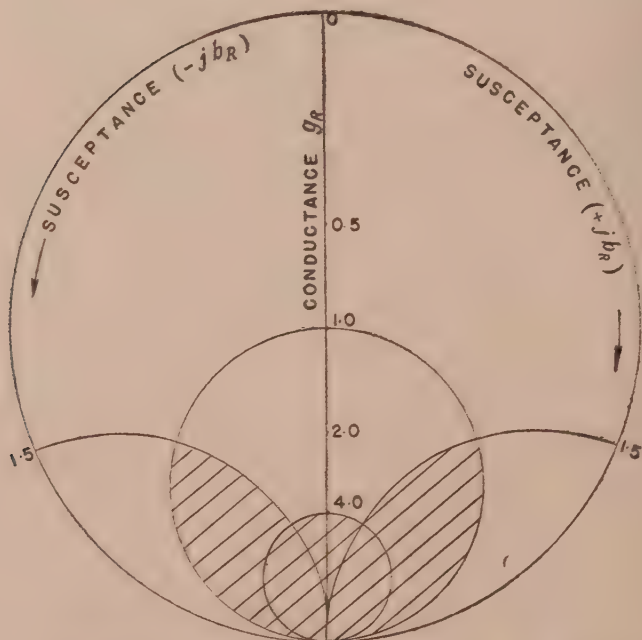


Fig. 5. Smith chart showing the range of impedance (shaded region) that can be matched.

Equ. (7) on simplification yields

$$\left. \begin{aligned} \cot \theta + \cot \theta' &= a \\ \operatorname{cosec} \theta + \operatorname{cosec} \theta' &= \pm b \end{aligned} \right\} \dots (8)$$

$$\text{where } a = b_R/(g_R - 1) \\ b = \sqrt{g_R(1 + a^2)}$$

The solutions of Equ. (8) are :

$$\left. \begin{aligned} \text{(i)} \quad \cot \frac{\theta}{2} &= \frac{1}{2} (d_1 \pm \sqrt{d_1^2 - 4c_1}), \quad \cot \frac{\theta'}{2} = \frac{1}{2} (d_1 \mp \sqrt{d_1^2 - 4c_1}) \\ \text{(ii)} \quad \cot \frac{\theta}{2} &= \frac{1}{2} (d_2 \pm \sqrt{d_2^2 - 4c_2}), \quad \cot \frac{\theta'}{2} = \frac{1}{2} (d_2 \mp \sqrt{d_2^2 - 4c_2}) \end{aligned} \right\} \dots (9)$$

$$\text{where } c_1 = (b+a)/(b-a), \quad c_2 = 1/c_1 \\ d_1 = a+b, \quad d_2 = a-b.$$

It can be easily shown that solutions for θ and θ' may also be obtained from the alternative forms of Eq. (8) given below in Eq. (10) and (11) :

$$\text{cosec}^2 \theta \mp b \text{ cosec } \theta + \left(\frac{a^2}{b^2 - a^2} + \frac{b^2 - a^2}{4} \right) = 0 \quad \left. \dots (10) \right\}$$

and an identical equation for $\text{cosec } \theta'$.

$$\cot^2 \theta - a \cot \theta + \left(\frac{b^2}{b^2 - a^2} - \frac{b^2 - a^2}{4} \right) = 0 \quad \left. \dots (11) \right\}$$

and an identical equation for $\cot \theta'$.

Physically realisable solutions for θ and θ' are obtained provided the inequality $g_R + b_R^2/(g_R - 1) \geq 4$ is satisfied. The range of y_R where it is possible to get an impedance match is thus shown by the shaded region in the Smith chart (Fig. 5). It would be seen that whenever load V.S.W.R. ≥ 4 , an impedance match at the input T -junction can always be obtained by locating the putput T -junction at any appropriate point inside the shaded region.

A similar analysis for the case when the characteristic admittances of lines A and B are each half the input and output lines, shows that all load V.S.W.R.'s can be matched.

V. S. W. R. IN EACH LINE

The normalised values of the output admittances y_{A0} and y_{B0} terminating the

lines A and B respectively (see Fig. 3), are dependent upon the line lengths and the load admittance and are given by

$$\begin{aligned} y_{A0} &= -(I_2/E_2) \\ &= \frac{y_{12}(y_R + y'_{22}) - y_{22}y'_{12}}{y_{12} + y'_{12}} \\ &= \frac{y_R \operatorname{cosec} \theta - j \operatorname{cosec} \theta \cot \theta' - j \cot \theta \operatorname{cosec} \theta'}{\operatorname{cosec} \theta + \operatorname{cosec} \theta'} \quad \dots (12) \end{aligned}$$

$$\begin{aligned} y_{B0} &= -(I'_2/E'_2) \\ &= \frac{y'_{12}(y_R + y_{22}) - y_{22}'y_{12}}{y_{12} + y'_{12}} \\ &= \frac{y_R \operatorname{cosec} \theta' - j \operatorname{cosec} \theta' \cot \theta + j \cot \theta' \operatorname{cosec} \theta}{\operatorname{cosec} \theta + \operatorname{cosec} \theta'} \quad \dots (13) \end{aligned}$$

In the above all admittances denoted by lower case symbols are normalised with respect to Y_0 .

Once the complex values of y_{A0} and y_{B0} are obtained from Eqns. (12) and (13), the reflection coefficients Γ_{A0} and Γ_{B0} at the output ends of lines A and B respectively are readily determined. Thus

$$\left. \begin{aligned} \Gamma_{A0} &= (1 - y_{A0})/(1 + y_{A0}) \\ \Gamma_{B0} &= (1 - y_{B0})/(1 + y_{B0}) \end{aligned} \right\} \quad \dots (14)$$

The V.S.W.R.'s set up in each line are then :

$$\left. \begin{aligned} \rho_A &= (1 + |\Gamma_{A0}|)/(1 - |\Gamma_{A0}|) \quad \text{for line } A \\ \rho_B &= (1 + |\Gamma_{B0}|)/(1 - |\Gamma_{B0}|) \quad \text{for line } B \end{aligned} \right\} \quad \dots (15)$$

SPECIAL CASE OF RESISTIVE LOADS ($g_R \geq 4$)

Let us consider the case when the load V.S.W.R. ≥ 4 . If now the load presented at the output T -junction is resistive, $b_R = 0$ and $y_R = g_R (\geq 4)$. For such a situation, assumed to be brought about by proper location of the matching device along the load side of the transmission line, Eqns. (8), (12) to (15) are very much simplified and are respectively given below :

$$\left. \begin{aligned} \cot \theta + \cot \theta' &= 0 \\ \operatorname{cosec} \theta + \operatorname{cosec} \theta' &= \pm b \\ \text{whence } \theta + \theta' &= \pi \\ \text{and } \operatorname{cosec} \theta &= \pm b/2 \end{aligned} \right\}$$

$$\left. \begin{aligned} y_{A0} &= (g_R/2) + j \cot \theta \\ y_{B0} &= (g_R/2) - j \cot \theta \end{aligned} \right\}$$

$$\Gamma_{A0} = \Gamma_{B0} = [(g_R - 3)/(g_R + 5)]^{\frac{1}{2}}$$

$$\rho_A = \rho_B = (\sqrt{g_R + 5} + \sqrt{g_R - 3})/(\sqrt{g_R + 5} - \sqrt{g_R - 3})$$

The last one shows that when the load V.S.W.R. $\gg 5$, ρ_A and ρ_B are each approximately half the load V.S.W.R.

EXPERIMENTAL VERIFICATION

Three re-entrant line matching sections were made with two *T*-junctions and lengths of rigid air dielectric coaxial lines (outer 5.8" OD \times 1.32" wall tubing and inner 0.244" dia) of characteristic impedance 50 ohms having the following electrical lengths :

- (i) $l = 26.34$ cm, $l' = 99.90$ cm
- (ii) $l = 16.34$ cm, $l' = 89.90$ cm.
- (iii) $l = 15.04$ cm, $l' = 89.90$ cm

Calculated performances of each of these when the output *T*-junction is placed at a voltage minimum (resistive load) show that the input should be matched at

- (i) $\lambda = 252.48$ cm, frequency = 118.82 Mc/s
when load V.S.W.R. = 10.75, i.e., $g_R = 10.75$
- (ii) $\lambda = 212.48$ cm, frequency = 141.19 Mc/s
when load V.S.W.R. = 18.51, i.e., $g_R = 18.51$
- (iii) $\lambda = 209.88$ cm, frequency = 142.94 Mc/s
When load V.S.W.R. = 21.13, i.e., $g_R = 21.13$

Measurement of admittance at the input *T*-junction with an U.H.F. Admittance Meter (General Radio Co., type 1602B) showed perfect agreement in each case within the accuracy of the instrument.

ACKNOWLEDGMENTS

Author's thanks are due to Prof. H. Rakshit and Mr. R. C. Ganguly for several helpful discussions.

SOME STUDIES ON THE SPREAD-F, DOUBLE-F AND FORKED-F TRACES AS OBSERVED AT HARINGHATA (CALCUTTA)

R. N. DATTA

INSTITUTE OF RADIOPHYSICS AND ELECTRONICS, UNIVERSITY OF CALCUTTA, CALCUTTA-9

(Received, August 19, 1960)

ABSTRACT. The paper deals with the occurrence and origin of the Spread-F phenomena including 'double' and 'forked' F-traces. From the spread-F records and from the theoretical relation of the spread-F index with the critical frequency and the velocity of irregularities, it is found that the percentage of occurrence of spread-F depends both on the electron density and the velocity of the irregularities. The night-time appearance of this phenomenon and its sharp decrease at sunrise lend support to this conclusion.

INTRODUCTION

Irregular and diffuse reflections from the night-time F layer, commonly known as the spread- F or F -scatter phenomena, have received considerable attention in recent years particularly in relation to its diurnal and seasonal variations and its dependence on magnetic activities. In this paper, a study of the spread- F phenomena has been made from the $h' - f$ records of Haringhata (Geomag. lat. 12.5°N , long. $88^\circ 31'\text{E}$, lat. $22^\circ 56'\text{N}$) for low sunspot years 1955-56, and the characteristics obtained at this latitude are compared with those reported from other places. Theoretical consideration on the origin of spread- F and its relation with F_2 region irregularities have been examined.

The study of the observed characteristics includes diurnal and seasonal variations of the nature and occurrences of spread- F in different seasons and on magnetically quiet and disturbed days. An index of scale zero to three as suggested by Briggs (1957) has been followed for indicating the degree of spreading (scale zero referring to normal trace and scales one, two and three to the weak, medium and intense types of scattering respectively). The relations between $f_0 F_2$ with the occurrence of spread- F and its latitude variation have also been discussed. A study of the nature and occurrences of double- F and forked- F traces has been made, as, both the said traces are usually found to precede or follow the scattering phenomena. According to Briggs (1957), the spread in critical frequency is due to the presence of the ionospheric irregularities in the F region and according to Voge (1955) these irregularities are dependent on the velocities. It is shown that if account is taken of both these factors, that is, when

the velocity term is included in the expression for the spread in critical frequency, the characteristics of the diurnal and seasonal variations are better understood.

CHARACTERISTICS OF THE SPREAD-F PHENOMENON

The night-time F echoes in the ionograms, leaving aside the simple traces can be classified broadly into three types : (a) Spread- F , (b) Double- F and (c) Forked- F traces (Fig. 1).

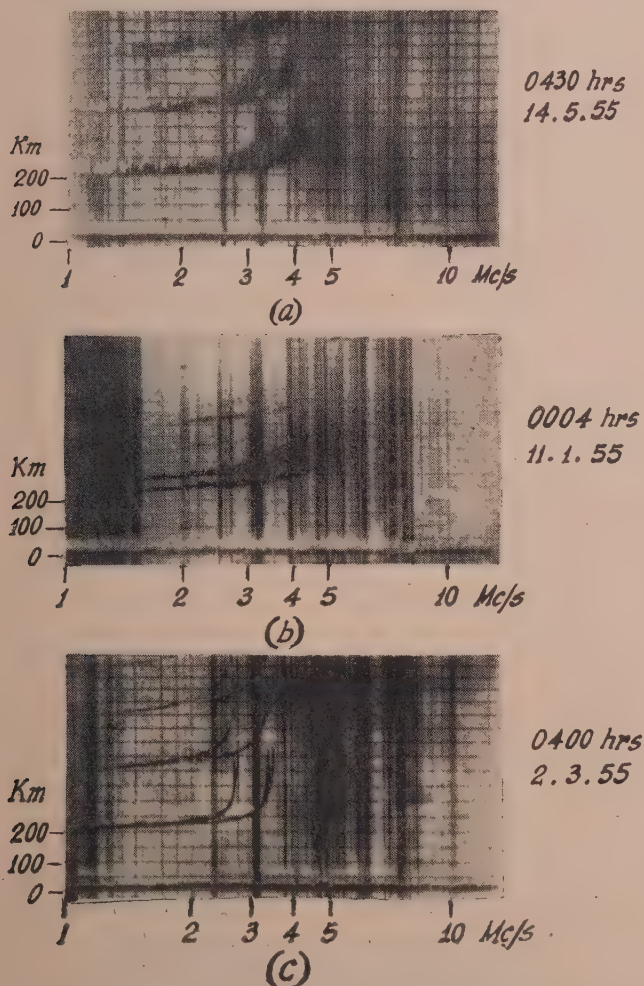


Fig. 1. Typical $h'-f$ record obtained at Haringnata showing
(a) Spread- F ,
(b) Double- F ,
and (c) Forked- F traces,

(a) *Spread- F trace*: This is a thickening and diffusiveness of both the O and X components of the regular F -echoes which become more marked near the critical frequencies. Appearing at any part of the night, usually some time after sunset, it becomes more prominent with the progress of the night and decays sharply at sunrise. During the same night the variation in the degree of the spread may pass through one or two peaks. The spread also exhibits seasonal variations in the frequency of occurrence. There is a general agreement in the diurnal variations in the degree of spread obtained at different stations, but the seasonal variations as reported from different places appear to be different. From the analysis of data done by Reber (1954), Briggs (1956), Kasuya *et al.* (1955), Wells (1954), Dagg (1957), Wright *et al.* (1956) and Lyon *et al.* (1958), it is found that leaving aside the auroral type of spreading, the characteristics of spread- F are of two types, namely, (i) middle or temperate latitude type and (ii) low latitude or equatorial type. The occurrences of temperate latitude type of spreading have a tendency to increase during winter whereas those of equatorial type increase during summer in low sunspot years. McNicol and Bowman (1957), after examining the data for a number of stations, observed that a reasonable smooth distribution of occurrences of spread- F exists in the range of geomagnetic latitudes between $20^{\circ}N$ or S and $45^{\circ}N$ or S , and that the existence of equatorial type is comparatively small. No suggestion for the change over latitude from equatorial to temperate latitude type of spreading has been given there. Lyon *et al.* (1958) from a study of spread- F and magnetic activity suggested, from the results of two stations, Karoia and Johannesburg, situated at the temperate latitudes, that the transition from equatorial to temperate type of spreading is at some latitude between these two stations and at about $20^{\circ}S$ (Geo. lat.) or $35^{\circ}S$ (Geomag. lat.). Recently Kotadia (1959) after examining the data of some northern stations has suggested the change over latitude to be at $31.2^{\circ}N$ (Geo. lat.). But the suggested belt for the types of spreading cannot explain the non-seasonal variation of the occurrence of spread- F at Washington ($50.3^{\circ}N$ Geomag. lat.) and at Rarotonga ($21.7^{\circ}S$ Geomag. lat.). In our case, however, it is found that percentage of occurrence of spread- F traces, of all the three degrees, is more marked in summer than in winter and is minimum during the *autumnal equinox*. The observational results are depicted in Figs. 2(a), (b), (c) and (d).

Hourly per cent counts of spread- F occurrence have been made separately for the magnetically quiet and disturbed days from the Haringhata data for the summer season in the low sunspot year 1955-56. Variations of the counts are shown in Fig. 3. It will be seen that percentage of occurrences is higher on the magnetically quiet than on the disturbed days. Similar effect, i.e., decreased scatter with increased magnetic activity, has been observed for summer at Ibadan (Geomag. lat. $10.4^{\circ}N$), Kodaikanal (Geomag. lat. $0.6^{\circ}N$), Singapore (Geomag. lat. $10^{\circ}S$) and Ahmedabad (Geomag. lat. $13.6^{\circ}N$).

Some anomalies also exist regarding the occurrence of spread- F echoes in relation to f_0F_2 . Reber (1954) at Hawaii found a clear inverse correlation, whereas Dagg (1957) did not find it as clearly at Slough. The night-time f_0F_2 and its association with spreading phenomena has been studied for Haringhata. The critical frequencies are grouped as shown in Table I and in each range of frequencies, percentage of occurrences of spread- F has been observed.

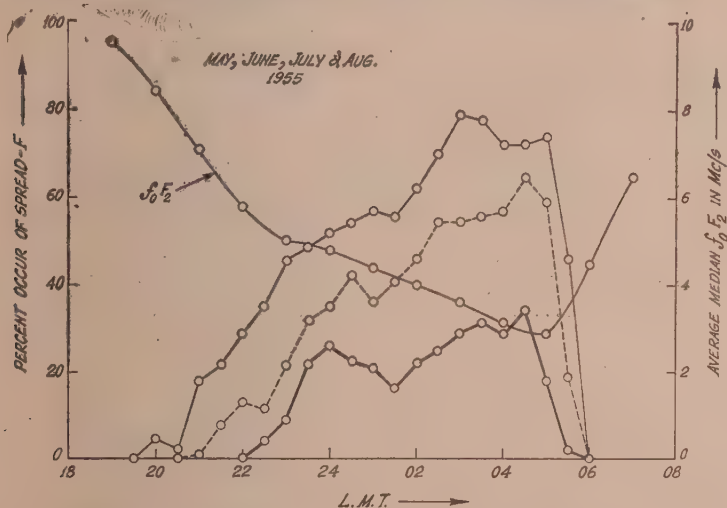


Fig. 2 (a). Diurnal variation of percent count of occurrences of spread- F in summer.
.....weak, — medium, — intense.

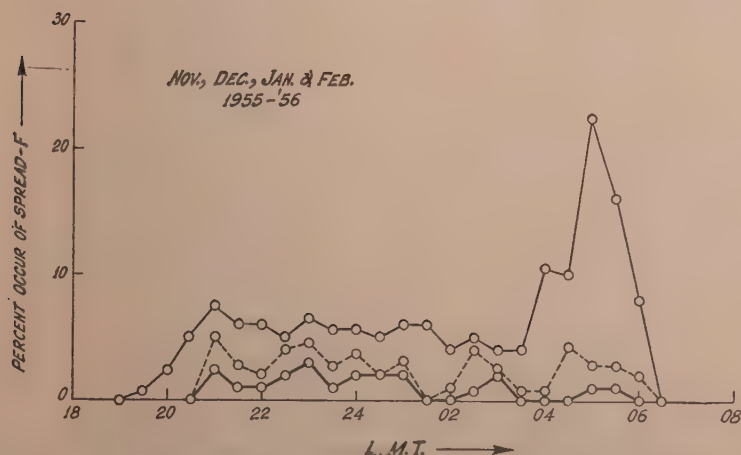


Fig. 2 (b). Diurnal variation of percent count of occurrences of spread- F in winter.
.....weak, — medium, — intense.

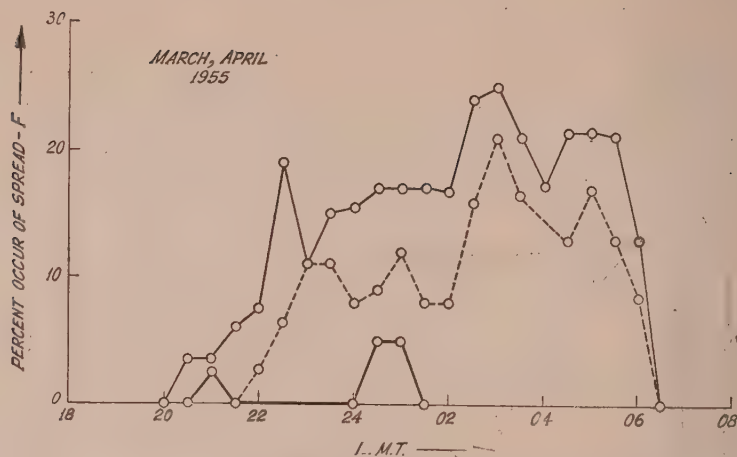


Fig. 2 (c). Diurnal variation of percent count of occurrences of spread- F , in vernal equinox.
 weak, — medium, ——— intense.

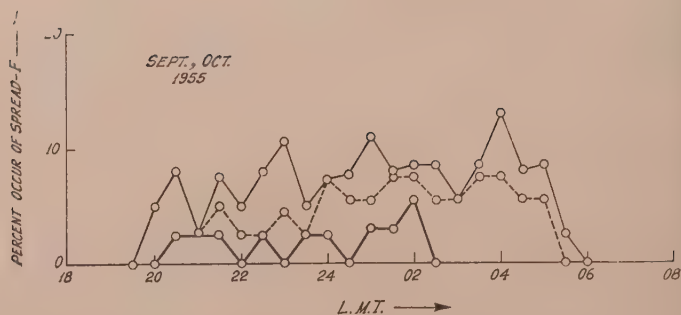


Fig. 2(d). Diurnal variation of percent count of occurrences of spread- F for Haringhata for the three different degree in autumnal equinox.
 weak, — medium, ——— intense.

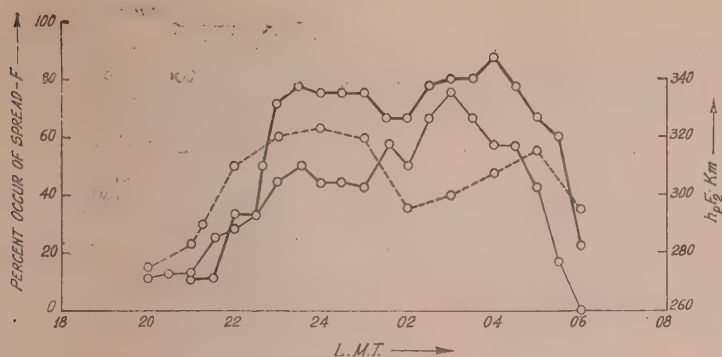


Fig. 3. Diurnal variation of percent count of occurrences of spread-F for magnetically quiet and disturbed days and variation of hourly median values of $h_p F_2$ at Haringhata. Heavy line represents mag. quiet days light line represents mag. disturbed days and dashed line represents $h_p F_2$.

TABLE I

Frequency range in Mc/s	Percentage of occurrence of spread F
1.5—2.0	84
2.1—2.5	80
2.6—3.0	75
3.1—3.5	71
3.6—4.0	45
4.2—4.5	27
4.5—5.0	30
5.1—5.5	11
5.6—6.0	2
6.0—7.0	0
7.0—8.0	0

The graph drawn from the above results in the form of histogram (Fig. 4), shows that percentage of spread-F becomes prominent as the critical frequency is lowered, and is thus a decreasing function of f_0 . The same conclusion can be drawn from Fig. 2(a), showing the nature of variation of percent count of spread-F with the hourly average median $f_0 F_2$. The ionograms for the summer months have only been taken for this analysis, as, during these days the missing records are least.

Variation of hourly median values of $h_p F_2$ and appearance of spread-F at Haringhata show that there is fairly parallel relationship between the two. Maximum of $h_p F_2$ coincides with the peak of the frequency of occurrence of spread-F (Fig. 3). The result supports those obtained by Kasuya *et al.* (1954) and Bowman (1960) and suggests that spread-F is originated from the upper F region.

(b) *Double F-traces* and (c) *Forked-F traces* : Night time $h' - f$ records sometimes contain two parallel F layer traces each showing the usual magnetoionic splitting with some degree of spreading. These are too close to each other to admit of any explanation in terms of multiple reflections. It is believed that the upper trace is due to oblique reflections from some moving folds or deformities in the F region.

Sometimes, instead of broadening, each of the two components of the F layer trace assumes a forked appearance near the critical frequency.

Typical examples of double- F and forked- F traces from our records are shown in Fig. 1(b) and 1(c).

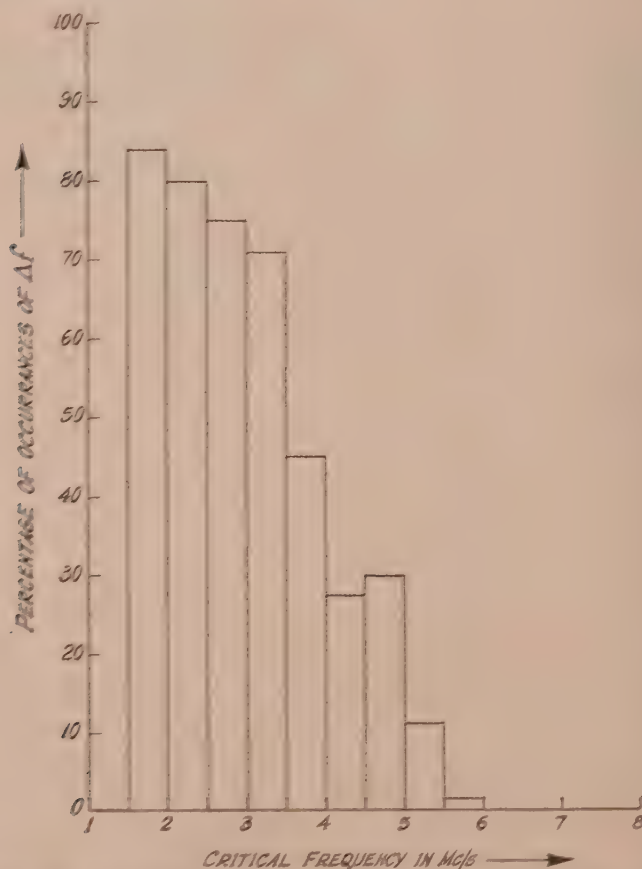


Fig. 4. Variation of percent count of occurrences of Spread- F with f_oF_2 for summer quiet days at Haringhata.

From the study of ionograms it is found that these are invariably associated with some degree of spreading either preceding or following the simple traces. Moreover, the diurnal variations of their occurrences for summer season (Fig. 5)

follow the same pattern as that of the spread-F occurrence. This suggests that the causes of spread-F, double-F and forked-F traces are likely to be the same, the particular picture depending probably on the size and orientation of the said irregularities.

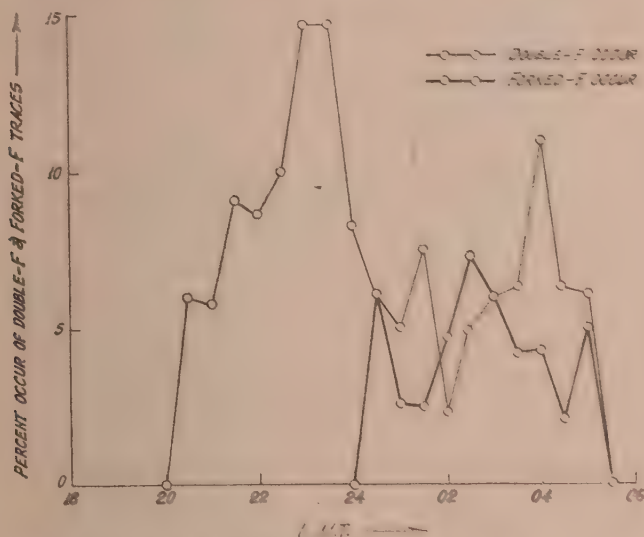


Fig. 5. Diurnal variation of double-F and forked-F traces for summer seasons as found at Haringhata.

THEORETICAL INTERPRETATION OF OBSERVATIONAL RESULTS

A considerable amount of work has been done to explain the observed characteristics of the Spread-F phenomenon. According to the present state of knowledge, the most prominent cause of the phenomenon appears to be the irregularities which are known to exist in the electron density distribution in the F region. These irregularities have been found to correlate positively with magnetic activity at high latitudes and negatively at low latitudes. According to the above hypothesis Spread-F condition should exhibit similar correlation with magnetic activity. This indeed is what is found from the observations of Hertz (1959) and Lyon *et al.* (1958) and also from our result.

The effect of irregularities on the spread-F has been examined theoretically by Briggs. According to this author, the relation between the irregularity ΔN , the critical frequency f_o , and the spread Δf_o , is given by

$$\Delta N \propto f_o \Delta f_o$$

Also, it has been shown by Voge (1955) that if v is the velocity with which the

irregularity is drifted then ΔN is proportional to v^2 . Hence, combining the above relation with Vege's proportionality

$$\Delta N \propto v^2$$

we may write

$$f_0 \Delta f_0 \propto v^2$$

or

$$\Delta f_0 \propto \frac{v^2}{f_0}, \text{ i.e., } \frac{v^2}{\sqrt{N}}$$

This shows that the night-time increase in velocities of the irregularities and simultaneous decrease in electron density can intensify the degree of spreading. That the velocity changes considerably is well known from the measurement of drift movement by radio astronomical techniques. Drift speeds of 60 m/sec at 19 hr, 290 m/sec at 01 hr and 170 m/sec at 05 hr, have been recorded (Maxwell, 1954). Moreover, the decrease in electron density may cause the enhancement of scattering, for, such decrease in electron density reduces the electromagnetic damping of the turbulence on which the production of the irregularities depends (Booker, 1958). It has been suggested (Booker and Wells, 1938; Maxwell, 1954; Martyn, 1955 and Dagg 1957) that the irregularities may have their origin in the E layer turbulence created in the Dynamo region at night, the turbulence effect being communicated to the F region by the presence of earth's magnetic field. It is to be noted that v in the term v^2/f_0 varies considerably at the same place and also from place to place. This may explain the anomalies of the seasonal variations of spread- F occurrences at different places. Also, Δf_0 depends inversely on f_0 . This inverse dependence may perhaps be associated with the observed relation of $f_0 F_2$ and the percentage occurrence of spread- F .

CONCLUDING REMARK

Occurrence of spread- F is a night-time phenomenon and becomes more prominent at Haringhata during summer, during magnetically quiet days and during periods of low critical frequency. The observed results are in agreement with those obtained at equatorial stations like Ibandan, Singapore and Ahmedabad during low sunspot years. The change over latitude from the temperature type of spread to the equatorial type is not yet definitely known. Washington (Geomag. lat. $50^\circ.3N$) and Rarotonga (Geomag. lat. $21.7^\circ S$) may lie in the change over region. The anomaly of clear inverse correlation of spread- F occurrence with critical frequency at different places may be attributed to the possible fluctuations in the velocity of the irregularities. The ionograms, where the spread in critical frequency is measurable accurately (as in the case of weak spreading), may be used to estimate the velocity of the irregularities from the observed critical frequency and its spreading.

ACKNOWLEDGMENTS

The work forms part of the programme of the Radio Research Committee of the Council of Scientific and Industrial Research, Government of India. The author is indebted to Professor J. N. Bhar, D.Sc., F.N.I., for his keen interest and encouragement. Thanks are also due to Dr. A. K. Saha for valuable suggestions.

REFERENCES

- Booker, H. G. and Wells, H. W., 1938, *Terr. Mag.*, **43**, 249.
 Booker, H. G., 1956, *J. Geophys. Res.*, **61**, 673.
 Booker, H. G., 1956, *J. Atmos. Terr. Phys.*, S. Suppl. Part II, **52**.
 Booker, H. G., 1958, *Proc. I.R.E.*, **46**, 298.
 Bowman, G. G., 1960, *Aust. J. Phys.*, **13**, 69.
 Briggs, B. H., 1957, *J. Atmos. Terr. Phys.*, **12**, 34.
 Briggs, B. H., 1957, *J. Atmos. Terr. Phys.*, **12**, 89.
 Dagg, M., 1957, *J. Atmos. Terr. Phys.*, **11**, 133 & 139.
 Eckersley, T. L., 1958, *Proc. Phys. Soc.*, **56**, 1025.
 Hartz, T. R., 1959, *Canadian Jour. of Phys.*, **37**, 1137.
 Kasuya, I., Kataho, S. and Taguhi, S., 1955, *J.R.R.L. (Japan)*, **2**, 329.
 Katodia, K. M., 1959, *Proc. Ind. Acad. of Sciences*, L.
 Lyon, A. J., Skinner, N. J. and Wright, R. W., 1958, *Nature*, **181**, 1724.
 Maxwell, A., 1954, *Phil. Mag.*, **45**, 1247.
 McNicol and Bowman, G. G., 1957, *Aust. J. Phys.*, **10**, 588.
 Reber, G., 1954, *J. Geophys. Res* **59**, 257 & 445.
 Voge, J., 1955, *L'Onde Electrique*, **35**, 565.
 Wells, H. W., 1954, *J. Geophys. Res.*, **59**, 273.
 Wright, R. W., Koster, J. R. and Skinner, N. J., 1956, *J. Atmos. Terr. Phys.*, **8**, 240.

APPENDIX

If ρ is the density of air at the ionospheric region producing scattering and N is the number of electrons per unit volume then

$$N \propto \rho$$

$$\text{Hence} \quad \frac{\Delta N}{N} = \frac{\Delta \rho}{\rho} \quad \dots (1)$$

For perfect gas, where fluctuation of temperature is negligible it can be written that

$$\frac{\Delta \rho}{\rho} \simeq \frac{\Delta p}{p} \quad \dots (2)$$

where p is the pressure of air at that region.

The variation of atmospheric temperature with height during daytime and night-time (Fig. 6) shows that temperature gradient at night is comparatively low. So the Eqn. (2) is applicable in the ionospheric region at night.

Now $\Delta p \propto v^2$ (Bernoulli's principle).

$$\Delta N \propto v^2$$

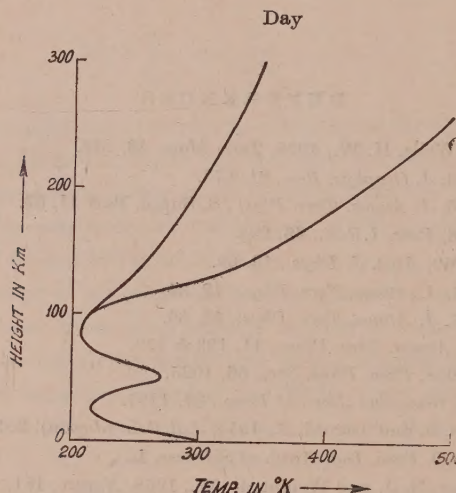


Fig. 6.

IMPORTANT PUBLICATIONS

The following special publications of the Indian Association for the Cultivation of Science, Jadavpur, Calcutta, are available at the prices shown against each of them:—

TITLE	AUTHOR	PRICE
Magnetism ... Report of the Symposium on Magnetism		Rs. 7 0 0
Iron Ores of India	... Dr. M. S. Krishnan	5 0 0
Earthquakes in the Himalayan Region	... Dr. S. K. Banerji	3 0 0
Methods in Scientific Research	.. Sir E. J. Russell	0 6 0
The Origin of the Planets	.. Sir James H. Jeans	0 6 0
Active Nitrogen— A New Theory.	.. Prof. S. K. Mitra	2 8 0
Theory of Valency and the Structure of Chemical Compounds.	.. Prof. P. Ray	3 0 0
Petroleum Resources of India	.. D. N. Wadia	2 8 0
The Role of the Electrical Double-layer in the Electro-Chemistry of Colloids.	.. J. N. Mukherjee	1 12 0
The Earth's Magnetism and its Changes	.. Prof. S. Chapman	1 0 0
Distribution of Anthocyanins	.. Robert Robinson	1 4 0
Lapinone, A New Antimalarial	.. Louis F. Fieser	1 0 0
Catalysts in Polymerization Reactions	.. H. Mark	1 8 0
Constitutional Problems Concerning Vat Dyes.	.. Dr. K. Venkataraman	1 0 0
Non-Aqueous Titration	.. Santi R. Palit, Mihir Nath Das and G. R. Somayajulu	3 0 0
Garnets and their Role in Nature	.. Sir Lewis L. Fermor	2 8 0

A discount of 25% is allowed to Booksellers and Agents.

N O T I C E

No claims will be allowed for copies of journal lost in the mail or otherwise unless such claims are received within 4 months of the date of issue.

RATES OF ADVERTISEMENTS

1. Ordinary pages:

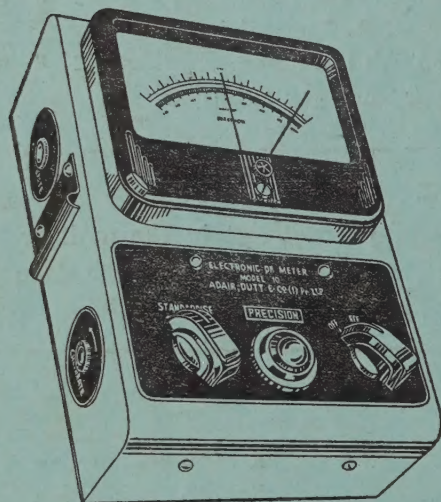
Full page	Rs. 50/- per insertion
Half page	Rs. 28/- per insertion
 2. Pages facing 1st inside cover, 2nd inside cover and first and last page of book matter:

Full page	Rs. 55/- per insertion
Half page	Rs. 30/- per insertion
 3. Cover pages

..	by negotiation
----	----	----	----	----------------
- 25% commissions are allowed to *bona fide* publicity agents securing orders for advertisements.

	PAGE
48. An Isotope Effect in the Collection on the Charged Plates of (n, γ) Recoil Products of Bromine—H. J. Arnikaar and A. Lal	441
49. Thermal Diffusion Factor for Hydrogen and Water Mixtures—S. C. Saxena	449
50. A Note on Heat Transfer and Film Boiling—R. D. Rao, H. S. Desai and D. V. Gogate	456
51. The Dielectric Properties of Copal Ester—A. K. Sen and G. N. Bhattacharya	461
52. The Lifetime of Hyperfragments—G. C. Deka	470
53. Impedance Matching by Re-entrant Stub Line—G. S. Sanyal	475
54. Some Studies on the Spread-F, Double-F and Forked-F Traces as Observed at Haringhata (Calcutta)—R. N. Datta	482

**'ADCO' 'PRECISION' MAINS OPERATED
ELECTRONIC pH METER MODEL 10**



Single range scale 0-14, continuous through neutral point.

Minimum scale reading 0.1 pH Eye estimation to 0.05 pH.

Parts are carefully selected and liberally rated.

Power supply 220 Volts, 40-60 cycles. Fully stabilised.

Fully tropicalized for trouble free operation in extreme moist climate.

SOLE AGENT

ADAIR, DUTT & CO. (INDIA) PRIVATE LIMITED
CALCUTTA. BOMBAY. NEW DELHI. MADRAS. SECUNDERABAD.

PRINTED BY KALIPADA MUKHERJEE, EKA PRESS, 204/1, B. T. ROAD, CALCUTTA-35
PUBLISHED BY THE REGISTRAR, INDIAN ASSOCIATION FOR THE CULTIVATION OF SCIENCE
2 & 3, LADY WILLINGDON ROAD, CALCUTTA-32